Osteohistological correlates of muscular attachment in terrestrial and freshwater Testudines

María Eugenia Pereyra,[1] [ID] Paula Bona,[1] Ignacio Alejandro Cerda[2] and Bárbara Desántolo[3]

[1]División Paleontología Vertebrados, Museo de La Plata (Unidad de Investigación Anexo), Facultad de Ciencias Naturales y Museo, CONICET, Buenos Aires, Argentina
[2]Instituto de Investigaciones en Paleobiología y Geología, Universidad Nacional de Río Negro y Museo Carlos Ameghino, CONICET, Cipolletti, Argentina
[3]Cátedra de Citología, Histología y Embriología A, Facultad de Ciencias Médicas, Universidad Nacional de La Plata, Buenos Aires, Argentina

Abstract

Sharpey's fibers are considered the anatomical structures integrated to the muscles. Since these fibers leave marks at the microscopic level, their presence and distribution are used as evidence of muscle attachment in extinct and extant forms. In recent years, studies have been focusing on muscle–bone and tendon–bone interaction mostly on mammals. The main objective of this work is to contribute to the morphological and histological knowledge of muscle attachment in other amniotes, such as reptiles, and their variation related to different locomotor habits. In this way, a study was performed on terrestrial and aquatic turtles. The musculature related to the movement of the humerus, and pectoral girdle in *Chelonoidis chilensis*, *Phrynops hilarii* and *Hydromedusa tectifera* was analyzed. Dissections were performed mapping the origins and insertions of each muscle and undecalcified thin sections were performed in specific muscular attachment sites. We found some differences which were not previously reported, related to the insertion of the *m. pectoralis*, the *m. coracobrachialis magnus* and the origin of the *m. tractor radii*. The osteohistology revealed the presence of Sharpey's fibers in the cortex of all the bone elements analyzed. Patterns were established in relation to the orientation and density of Sharpey's fibers, which were used for the categorization of each muscle attachment site. The comparative micro-anatomical study of these areas did not reveal any important differences between terrestrial and freshwater turtles in muscles involved with the rotation, abduction and adduction of the humerus. In this way, the preliminary results suggest an absence of correlation between the distribution and density of Sharpey's fibers between different habitat forms, at least in the bones and species analyzed.

Key words: osteohistology; Sharpey's fibers; Testudines.

Introduction

The anatomical knowledge about locomotion structures, such as the musculature and muscular attachment (e.g. bone–tendon interphase), is important within functional morphology. Among Testudines, Walker (1973) provides the most complete comparative analysis between cryptodiran and pleurodiran limb musculature, focusing on the relation between the anatomical variation and the different modes of locomotion (aquatic, semi-aquatic and terrestrial). Beyond this, only a few anatomical descriptions dealing with turtle limb musculature are available (Wyneken & Witherington, 2001; Abdala et al. 2008).

It has been shown that the tendon–bone insertion is complex (in terms of composition, structure and mechanical behavior) and well designed to transmit stress from tendon to bone (Trotter, 2002; Thomopoulos et al. 2010). The functioning and attachment of the muscles and tendons have a potential influence on the bone morphology. The bone responds to extrinsic forces that modify its shape. The stimulation of osteogenesis and consequent formation of bone tubers and ridges is due to the direct force exerted by the muscle (Washburn, 1947; Scott, 1957; Avis, 1959; Felts, 1959; Hoyte & Enlow, 1966; Moss, 1971; Hieronymus, 2002).

In recent years several studies have been conducted on the union of muscles to bones (Biermann, 1957; Benjamin et al. 1986, 2002; Suzuki et al. 2002, 2003; Hieronymus, 2006; Aaron, 2012; Petermann & Sander, 2013). In these

studies, different classifications and denominations of the muscle–bone interface have been used. Therefore, it is difficult to match the classifications because in many cases the criteria are not shared or are excluding. Here we follow Hieronymus (2006) and Benjamin et al. (2002) that there are two ways in which a muscle joins to the bone: with and without ligament or tendon. The former is called a tendon attachment and the latter a fleshy attachment. Also, the tendon attachment could be formed by fibrocartilaginous or fibrous entheses (Cooper et al. 1970; Benjamin et al. 1986, 2002; Hieronymus, 2006). It is known that the entheses transmit the contractile force generated by the muscle (Benjamin et al. 2002). The mineralized fibers that are present in the fibrocartilaginous and fibrous entheses are interpreted as extrinsic fibers or Sharpey's fibers (Benjamin et al. 2002; Hieronymus, 2006). Also, it has been established that the fleshy attachment does not present extrinsic fibers (Hieronymus, 2006).

Sharpey's fibers are bundles of collagen fibers which are commonly involved in the musculoskeletal attachment, penetrating perpendicularly or at smaller angles to the cortex of the bone (Jones & Boyde, 1974; Francillon-Vieillot et al. 1990; Hieronymus, 2002; Aaron, 2012). Sharpey's fibers are established as the only continuous anatomical structures which are directly integrated with muscles, ligaments and tendons (Aaron, 2012). Sharpey's fibers remain embedded in the new bone deposition as the bone grows (Hoyte & Enlow, 1966). Extrinsic density of fibers, which is dependent on the stress exerted on the muscle attachment site, is higher in tendinous than in fleshy attachments (Boyde, 1972; Jones & Boyde, 1974; Hieronymus, 2002, 2006; Sanchez et al. 2013). It can also be highlighted that the fibrocartilaginous entheses present a larger density of extrinsic fibers compared with the fibrous entheses (Matyas et al. 1990; Hems & Tillmann, 2000; Staszyk & Gasse, 2001; Sanchez et al. 2013). The distinction between the two types of attachment leads us to make hypotheses about the stresses in different parts of the musculoskeletal system of extinct organisms (Sanchez et al. 2013).

In general, most of the works that analyze Sharpey's fibers in relation to the attachment muscles are made using the decalcification of the bones as the main methodology (e.g. Cooper et al. 1970; Benjamin et al. 1986, 2002; Benjamin & Ralphs, 1997; Suzuki et al. 2002, 2003; Hieronymus, 2006). Some authors have begun processing mineralized bones to carry out their studies (Petermann & Sander, 2013). This methodology brings with it the advantage of being able to make comparisons between extant and extinct organisms, as the inorganic material is what is generally left in fossil organisms. In this way, paleobiological inferences contribute to the knowledge and understanding of the fauna found in the fossil record.

Several authors have studied the bone–tendon or bone–ligament interaction at a microanatomical level (e.g.

Benjamin et al. 2002; Suzuki et al. 2002, 2003; Hieronymus, 2006; Aaron, 2012; Petermann & Sander, 2013). In general, these studies have focused on the histological characteristics related to the muscle attachment (Benjamin et al. 2002; Suzuki et al. 2002, 2003; Sanchez et al. 2013), on the modifications that can be found during bone development (Hurov, 1986) and on the modifications that can be linked due to the force exerted by the muscles on the bones (Washburn, 1947; Scott, 1957; Avis, 1959; Felts, 1959; Hoyte & Enlow, 1966; Moss, 1971; Hieronymus, 2002). These studies have mostly been done in mammals and less in reptiles; among sauropsids, the analysis of muscle insertions reflected at the level of bone microstructure in turtles has not as yet been reported.

A comprehensive myological description of the pectoral girdle and forelimb of cryptodiran (*Chelonoidis chilensis*) and pleurodiran (*Hydromedusa tectifera* and *Phrynops hilarii*) turtles are performed here. Since muscle development and function varies according to different locomotor habits, it is expected that the histological features related to these muscles also varies. In this way we have determined the origin and insertion sites of the pectoral girdle and the stylopodium of the forelimb of *C. chilensis*, *H. tectifera* and *P. hilarii*; establishing which entheses leave osteohistological marks; characterizing the bone histology of the entheses at the origin and insertion sites; and determining the main osteohistological variations between different types of entheses. The main goal of this work is to provide new information regarding morphology and histology of the forelimb entheses of these cryptodiran and pleurodiran turtles and to explore whether differences between the same type of entheses occur in taxa with different locomotor habits.

Institutional abbreviations

MLPR, herpetological collection of the Museo de La Plata, La Plata, Buenos Aires Province, Argentina; AC, Laboratory of Anatomía Comparada of the Facultad de Ciencias Naturales y Museo, La Plata, Buenos Aires Province, Argentina; CH, Laboratory of Herpetology of the Facultad de Ciencias Naturales y Museo, La Plata, Buenos Aires Province, Argentina.

Material and methods

Eight specimens of three taxa were examined in this study, including *C. chilensis* (three individuals), *H. tectifera* (three individuals) and *P. hilarii* (two individuals; Table 1). All the examined specimens are housed in the herpetological Collection of the Museo de La Plata, in the Laboratory of Comparative Anatomy of Vertebrates of Facultad de Ciencias Naturales y Museo, La Plata and in the Laboratory of Herpetology of the Facultad de Ciencias Naturales y Museo, La Plata (Table 1). The specimens were found dead, some in fresh conditions and others dry. All were adults and sexed, except MLPR 6502, which could not be sexed.

Table 1 Specimens and skeletal bones examined for myology and histology.

Species	Sex	Total length (cm)	Condition of the material	Dissection	Thin section
Phrynops hilarii (MLP R 6402)	Male	29.8	Fresh	Whole left forelimb	Whole right forelimb
Phrynops hilarii (MLP R 6475)	Female	–	Fresh	Whole left forelimb	–
Hydromedusa tectifera (MLP R 6376)	Female	21.4	Fresh	Whole left forelimb	Left scapula
Hydromedusa tectifera (MLP R 6502)	–	11.9	Fresh	Whole right forelimb	–
Hydromedusa tectifera (MLP R 6411)	Male	21	Dry	–	Right humerus
Chelonoidis chilensis (AC)	Male	21	Dry	Whole left forelimb	Whole right forelimb
Chelonoidis chilensis (MLP R 6461)	Female	18.6	Fresh	Whole left forelimb	–
Chelonoidis chilensis (CH)	Female	29	Fresh	Whole left forelimb	–

Anatomy and dissection

The interpretation of the appendicular muscles during the dissections was performed following Walker (1973) and Abdala et al. (2008). We ordered the description of the muscles accordingly with their appearance, from the most superficial to the deepest ones. The terminology used for the descriptions is based on Walker (1973). Myological descriptions mainly focused on the differences among the studied taxa. Comparisons with other taxa [as *Pseudemys scripta elegans*; today *Trachemys scripta elegans* (Wied 1839)] were based on the bibliography (Walker, 1973). As opposed to Walker (1973), we consider the medial process of the humerus the one that is located towards the sagittal axis of the body, and the lateral process of the humerus the one located on the opposite side.

Some of the individuals used to analyze the musculature were frozen until the dissection and then were thawed at room temperature before examination; others were fixed in formaldehyde and preserved in alcohol 70 before dissections. The analysis was focused on the intrinsic muscles (attaching appendicular elements) involved in the movements of the stylopodium and zeugopodium, paying special attention to muscle attachments (origin and insertion), as well as to the structure and position of associated tendons. The appendicular musculature was first dissected to ascertain the location and extent of muscle attachments. The type of muscle attachment (tendinous or direct) was determined by gross observation. Areas of attachment on cleaned elements were digitally photographed.

Thin sectioning

Sharpey's fibers are traditionally observed in samples of decalcified bones (Cooper et al. 1970; Benjamin et al. 1986, 2002; Benjamin & Ralphs, 1997; Suzuki et al. 2002, 2003; Hieronymus, 2006). In recent times the use of propagation phase contrast X-ray synchrotron microtomography (PPC-SRmCT) has been established as a new methodology (Sanchez et al. 2013). However, here we use the technique for mineralized bones (Petermann & Sander, 2013) for the study of bone muscle attachments in extant and fossil individuals. We take into account the different attachment types, as well as different densities and distribution of extrinsic fibers.

The left or right humerus, scapula and coracoid of each individual was removed (Table 1), boiled with detergent solution and air-dried. Prior to sectioning, each bone was photographed and measured. In the humerus, three sections transverse to the element main axis were performed: on the proximal and distal metaphysis according to the muscle attachments and one on the shaft (at the growth center *sensu* Nakajima et al. 2014; Fig. 1). In the pectoral girdle, the histological slices were sectioned along one transverse plane in each girdle element. In each element, the slice was made a third of the way from the glenoid cavity to the extreme of each element (Fig. 1).

The thin sectioning was performed following standard petrographic procedures (Chinsamy & Raath, 1992). The thin sections were examined by polarized and ordinary light with $4\times$, $10\times$ and $20\times$ objectives using a petrographic microscope (Nikon Optiphot-Pol 255884) and under either polarizer 530 nm or 1/4 lambda plate. Images were obtained with digital camera (Smartphone Samsung S6 edge). The inclination angle of the Sharpey's fibers with regard to the subperiosteal (Fig. 1E) margin was obtained with ImageJ program (Rasband, 2003). In each region where Sharpey's fibers were observed, 10 measurements of angles of inclination were taken. In the Result section the highest and lowest values of each region were set. To analyze the abundance/density of fibers we followed the following criteria: we considered that the fibers are less abundant/dense when they are isolated and widely spaced from each other; and that they are abundant/dense when the fibers are not apart and in packages of more than 10 fibers. Nomenclature and definitions of histological structures used in this study are derived from Francillon-Vieillot et al. (1990).

To perform the analysis of the possible correlation between the attachment (insertion or origin) of the appendicular muscles and the patterns found in their microanatomy, we dissected each of the specimens and mapped the attachment of the muscles. This study was done using photographs and videos to be able to get as close as possible to the specific area of attachment. The videos with audios are useful and complementary to photograph because they give us an accurate picture of the dissection and a three-dimensional (3D) idea of the anatomical structures. It is important to note that some insertions or muscular origins are closely related (or contiguous) with each other, therefore it cannot be determined with certainty which muscle the microanatomical correlate corresponds to.

Results

Musculature description

The extrinsic muscles are not considered part of the appendicular apparatus (Walker, 1973; Figs 2–5). In spite of that, there are at least two muscles that have their insertions in
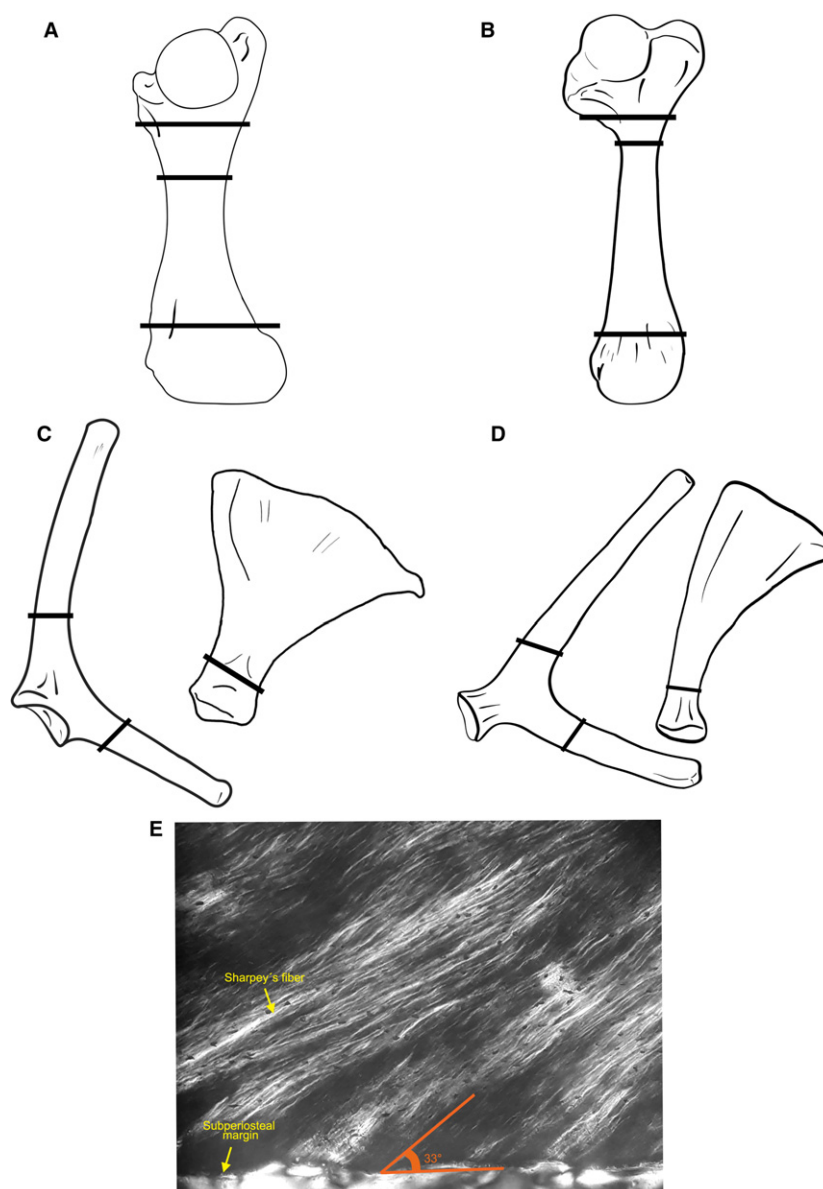
Fig. 1 Methodological steps. (A–D) Schematic drawing showing the position where of the thin sections were obtained in each element: *Chelonoidis chilensis* (A) humerus, (C) scapula and coracoid. *Phrynops hilarii* and *Hydromedusa tectifera* (B) humerus, (D) scapula and coracoid. (E) Measurement of the inclination angles of Sharpey's fibers.

the pectoral girdle that we could recognize only in *P. hilarii* and in *H. tectifera*:

Musculus testocoracoideus and *Musculus coracohyoideus*. The *m. testocoracoideus* insert in the medial surface of the scapular blade and in the dorsal surface of the coracoid; and the *m. coracohyoideus* inserts in the dorsal surface of the coracoid, proximal to the glenoid cavity (Figs 2A,E and 4A).

Musculus latissimus dorsi + musculus teres major. These are superficial muscles that insert together with a common

tendon on the dorsal surface of the proximal metaphysis of the humerus in all three taxa (Figs 3A,B and 4B). Because of the previous mechanical disarticulation of the limb, the origin points given in the carapace could not be observed when preparing the material. However, the fleshy origin of the *m. teres major* could be observed on the half end and anterior surface of the scapular blade in *P. hilarii* and *H. tectifera* (Fig. 2A), as reported in *Trachemys*, *Pelomedusa* and *Chelodina* (Walker, 1973); and only at the distal end of the anterior surface of the scapular blade in *C. chilensis* (Fig. 2B), as reported in *Dermochelys* and *Emys* (Walker, 1973). These muscles are described as abductors and
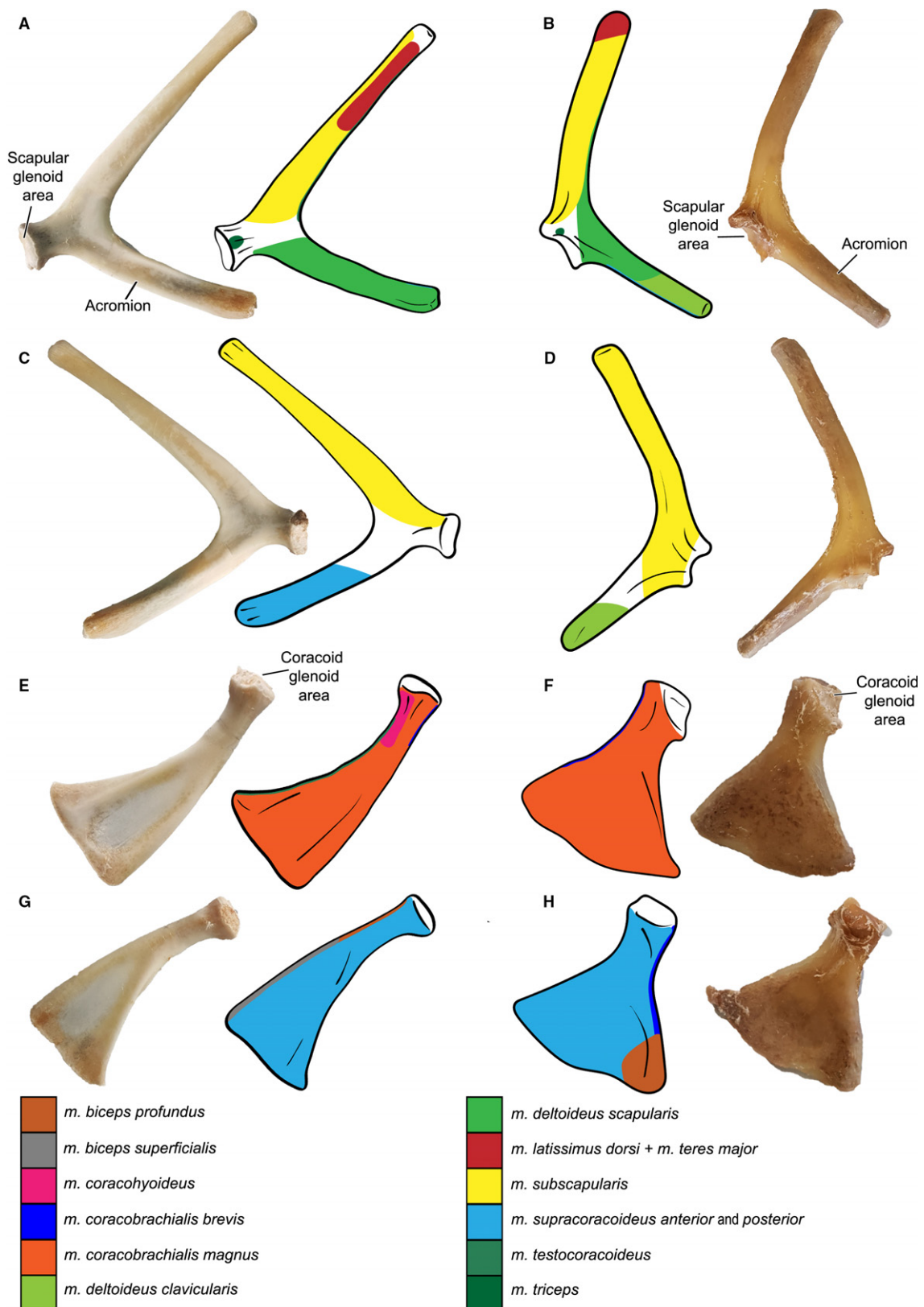
Fig. 2 Mapped muscle attachment sites. (A,C) Scapula of *Phrynops hilarii and Hydromedusa tectifera* in anterior and posterior view respectively. (E,G) Coracoid of *P. hilarii* and *H. tectifera* in dorsal and ventral view, respectively. (B,D) Scapula of *Chelonoidis chilensis* in anterior and posterior view, respectively. (F,H) Coracoid of *Chelonoidis chilensis* in dorsal and ventral view, respectively.
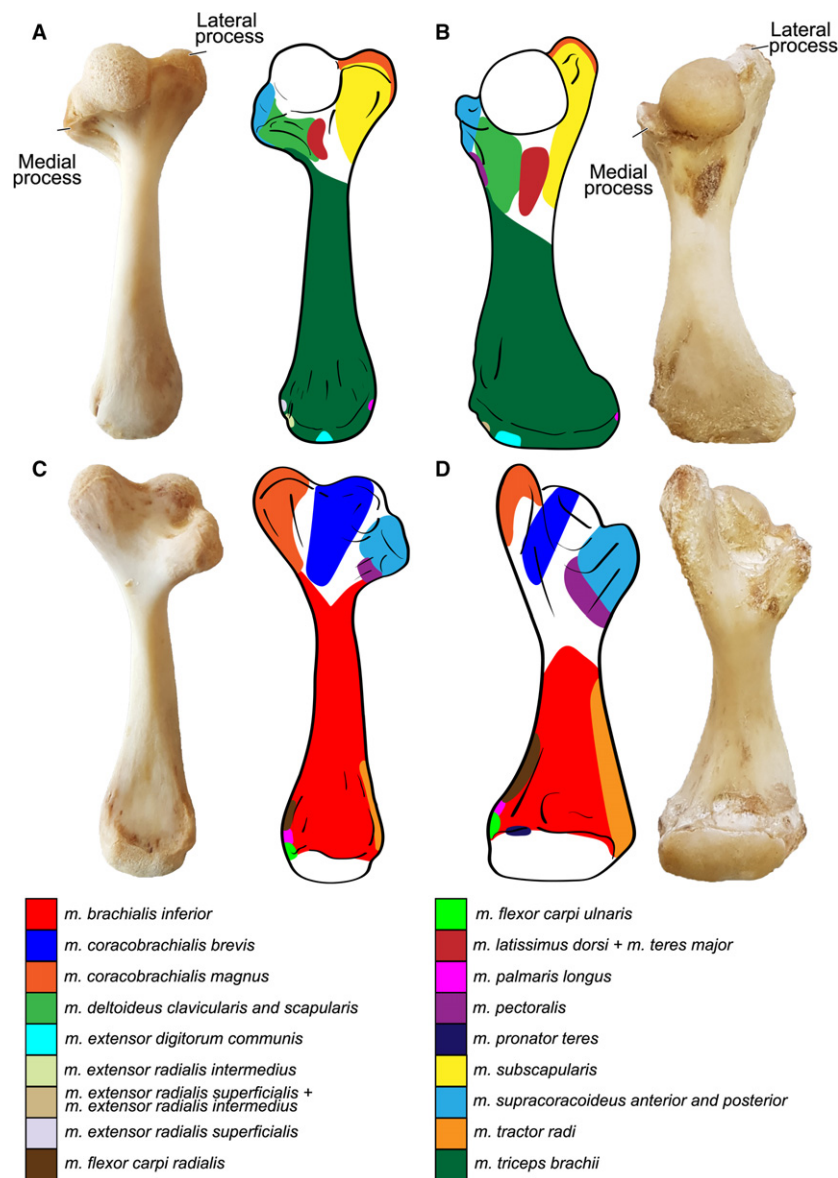
Fig. 3 Mapped muscle attachment sites. (A,C) Left humerus of *Phrynops hilarii and Hydromedusa tectifera* (in dorsal and ventral view, respectively). (B,D) Left humerus of *Chelonoidis chilensis* (in dorsal and ventral view, respectively).

protractors of the humerus. The *m. latissimus dorsi* is also involved in the anterior rotation of the pectoral girdle during the protraction of the limb (Walker, 1973).

Musculus deltoideus. This muscle is mostly observed in ventral view, but a little part is exposed in anterior view (Figs 4B–D and 5A). This muscle has two heads, the clavicular and the scapular head (Walker, 1973). In *P. hilarii* and *H. tectifera,* the two heads are not clearly divided and it is observed that the muscle arises from the anterior surface of the acromion (Figs 2A and 4C,D). However, in *C. chilensis* the scapular head arises medially from the scapular blade and anteriorly from the first portion of the acromion (Fig. 2B,D). The clavicular head arises distally from the

posterodorsal surface of the acromion and continues diagonally to the anterior surface of the acromion (Fig. 2B,D). In *Trachemys* the origin of this muscle is also at the medial portion of the epiplastron and adjacent parts of the entoplastron (Walker, 1973). However, as with the *m. latissimus dorsi* and *m. teres major*, the attachment of this muscle with the plastron could not be observed in the species studied here due to the previous mechanical disarticulation of the limb. In the three species examined here, the *m. deltoideus* inserts in the dorsal surface of the medial process of the humerus (Figs 3A,B and 4B,D). In *P. hilarii* and *H. tectifera* this muscle has a tendinous insertion, whereas in *C. chilensis* the type of insertion is fleshy. The *m. deltoideus* is an abductor and protractor of the humerus and probably
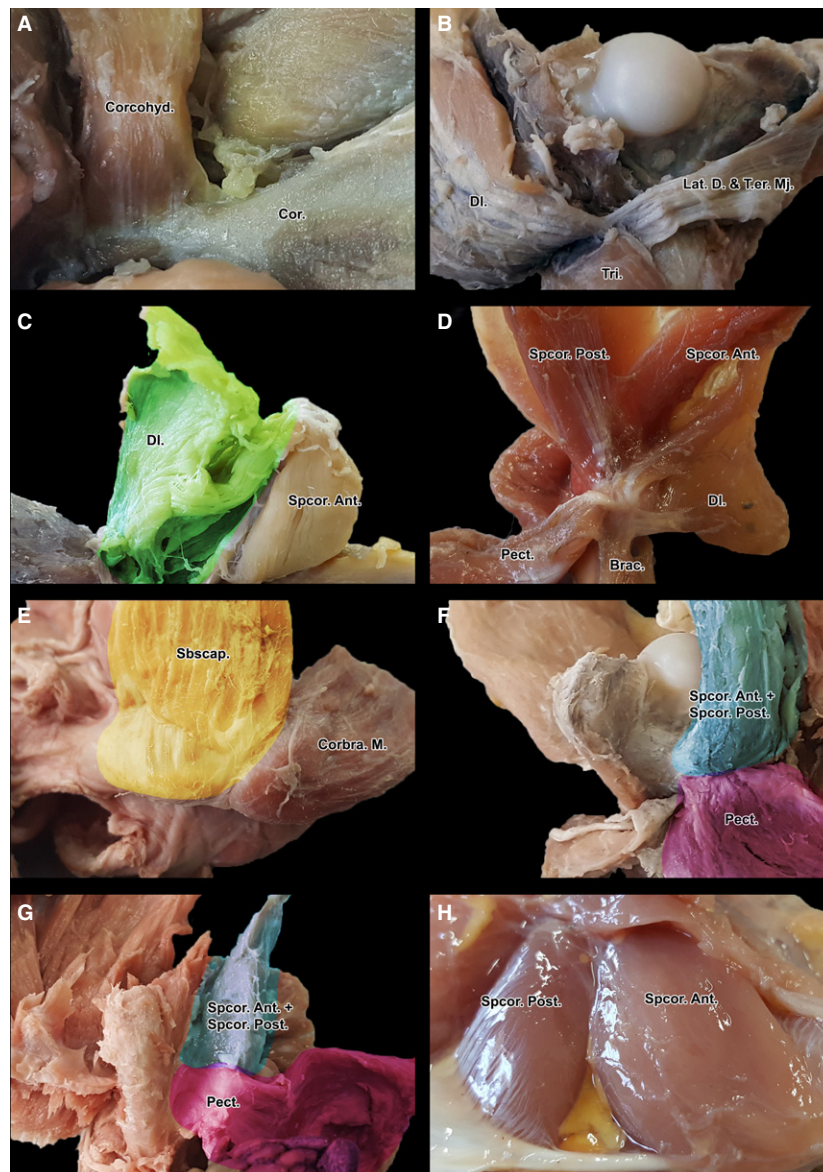
Fig. 4 Muscles dissected: (A) left coracoid of *Phrynops hilarii* (MLPR 6475), dorsal view; (B) left humerus of *P. hilarii* (MLPR 6475), dorsal view; (C) left acromion of *P. hilarii* (MLPR 6475), dorsal view; (D) left pectoral girdle of *Hydromedusa tectifera* (MLPR 6375), ventral view. (E) left humerus of *Chelonoidis chilensis* (CH), lateral view; (F) left humerus of *P. hilarii* (MLPR 6475), ventral view; (G) left humerus of *C. chilensis* (CH), ventral view; (H) left pectoral girdle of *P. hilarii* (MLPR 6402), dorsal view. Brac., brachialis inferior; Cor., coracoid; corbra. M., coracobrachialis magnus; Corcohyd., coracohyoideus; Dl., deltoideus; Lat. D. & Ter. Mj., latissimus dorsi and teres major; Tri., Triceps brachii; Sbscap., subscapularis; Spcor. Post., supracoracoideus posterior; Spcor. Ant., supracoracoideus anterior; Pect., pectoralis.

plays an important role in the anterior rotation of the entire pectoral girdle during limb protraction (Walker, 1973).

Musculus subscapularis. In *P. hilarii* and *H. tectifera*, this this muscle arises fleshy from the posterior and lateral surface of the scapular blade, and from the proximal half of the anterior surface (Fig. 2A,C). The *m. subscapularis* covers the entire length of the anterior, posterior and lateral surfaces of the scapula blade in *C. chilensis*; in this species it

also arises from the posterior surface of the proximal third of the acromion (Fig. 2B,D). The *m. subscapularis* inserts as a fleshy muscle in the dorsal surface of the lateral process of the humerus in the three species examined (Figs 3A,B and 4E). This muscle is described as a powerful abductor of the arm but probably also acts as a protractor of the limb (Walker, 1973).

Musculus triceps brachii. This muscle is extended along the dorsal surface of the humerus. It is a bulky muscle
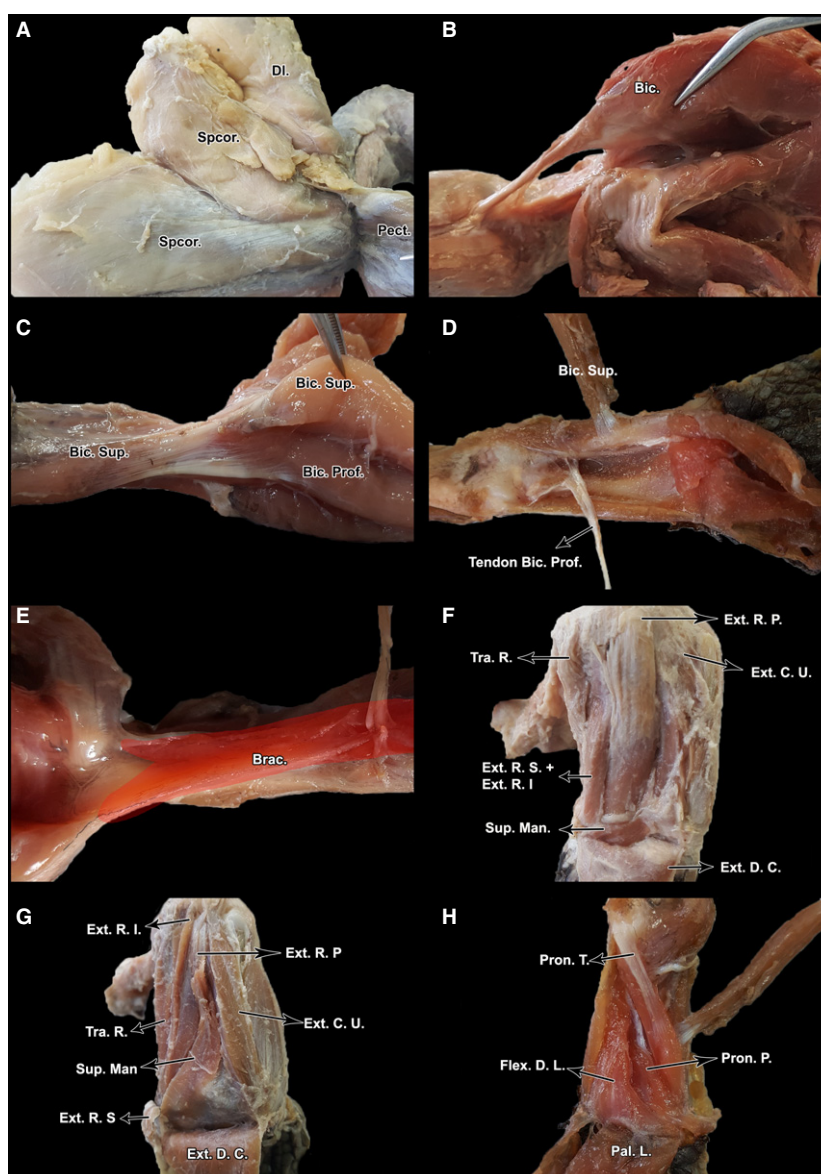
Fig. 5 Muscles dissected: (A) left pectoral girdle of *Phrynops hilarii* (MLPR 6475), ventral view; (B) left humerus of *Chelonoidis chilensis* (CH), ventral view; (C) left humerus of *P. hilarii* (MLPR 6402), posterior view; (D) left limb of *Hydromedusa tectifera* (MLPR 6376), ventral view; (E) left humerus of *P. hilarii* (MLPR 6402), ventral view; (F) left limb of *P. hilarii* (MLPR 6475), dorsal view; (G) left limb of *H. tectifera* (MLPR 6376), ventral view; (H) left limb of *C. chilensis* (CH), dorsal view. Brac., brachialis inferior; Bic., biceps; Bic. Prof., biceps profundus; Bic. Sup., bíceps superficialis; Dl., deltoideus; Ext. C. U., extensor carpi ulnaris; Ext. D. C., extensor digitorum communis; Ext. R. I., extensor radialis intermedius; Ext. R. P. extensor radialis profundus; Ext. R. S., Extensor radialis superficialis; Flex. D. L., flexor digitorum longus; Pect., pectoralis; Pron. P., pronator profundus; Pron. T., pronator teres; Sup. Man., supinator manus; Spcor., supracoracoideus; Tra. R., tractor radii.

consisting of two major bodies, one more superficial than the other. The superficial portion (scapular head *sensu* Walker, 1973) arises by a tendon which attaches on the scapula, dorsally to the glenoid cavity in the three species examined here (Fig. 2A,B). The underlying portion of this muscle (humeral head *sensu* Walker, 1973) arises fleshy from the proximal portion of the dorsal surface of the humerus, where in *P. hilarii*, *H. tectifera* and *C. chilensis* it is strongly adhered to Proximally, this head starts dorsolaterally and becomes dorsal at the shaft of the humerus

(Fig. 3A,B). The two portions of these muscles merge into a common tendon which inserts into the dorsal surface of the proximal end (olecranon) of ulna. The *m. triceps brachii* is the primary flexor of the antebrachium, but its scapular head can also act in protraction and abduction of the humerus (Walker, 1973).

Musculus pectoralis. This large muscle is composed of two bodies, the *m. pectoralis major* (posterior) and the *m. pectoralis minor* (anterior). According to Walker (1973), in

Trachemys this muscle arises from the anterior portion of the plastron; its attachment forms an arc that begins at the middle-ventral line, just posterior to the plastral attachment of the acromion, and extends posteriorly and laterally to the posterior boundary of the carapace bridge. The bodies of the *m. pectoralis* converge into a common tendon that inserts ventrally in the proximal metaphysis of the humerus. In *P. hilarii* and *H. tectifera* this tendon attaches just distal to the medial process of the humerus (Figs 3C and 4F). In *C. chilensis,* the insertion of the *m. pectoralis* is wider, occupying part of the ventral and medial surface of the medial process (Figs 3B,D and 4G). This muscle is an important retractor and adductor of the humerus and probably also plays a role in the posterior rotation of the girdle (Walker, 1973).

Musculus supracoracoideus. This muscle, which lies deep to the *m. pectoralis*, has two portions (anterior and posterior) occupying the whole triangular area between the acromion, the coracoid and the acromiocoracoid ligament (Figs 4D,H and 5A). The fleshy origin of this muscle varies slightly in turtles: its anterior portion arises from the ventral and posterior surface of the acromion and adjacent parts of the acromiocoracoid ligament in *Trachemys* (Walker, 1973); from parts of the ventral, posterior and parts of the dorsal surface of the acromion and adjacent parts of the acromiocoracoid ligament in *P. hilarii* and in *H. tectifera* (Figs 2C and 4C), but only from the ventral surface of the acromion and adjacent parts of the acromiocoracoid ligament in *C. chilensis*. The posterior portion of this muscle arises from the anterior and ventral surface of the coracoid (Fig. 2G,H) and adjacent parts of the acromiocoracoid ligament in all the turtles examined here (see also Walker, 1973). The two fleshy portions insert in the medial process of the humerus, invading the dorsal and ventral surface of this process (Figs 3A–D and 4F,G). The *m. supracoracoideus* is a retractor and adductor of the humerus, and probably is a protractor of the limb (Walker, 1973).

Musculus coracobrachialis magnus. This is a bulky muscle in all the turtles examined. It arises as a fleshy attachment from the dorsal surface of the coracoid (Fig. 2E,F) to insert also as a fleshy attachment at the lateral process of the humerus in the three species examined with some variations. In *P. hilarii* and in *H. tectifera*, the insertion of this muscle is extended along the ventral surface of the process (Fig. 3A,C). On the other hand, its insertion is extended less to the dorsal and ventral surface of the process in *C. chilensis* (Figs 3B,D and 4E). The *m. coracobrachialis magnus* is a retractor of the humerus and probably plays some role in humeral abduction (Walker, 1973).

Musculus coracobrachialis brevis. This muscle is located deep at the *m. coracobrachialis magnus*. It arises as a fleshy attachment from the posterior and part of the dorsal surface of the coracoid near to the glenoid fossa in *P. hilarii* and *H. tectifera* (Fig. 2E), and from almost the entire posterior and part of the ventral surface of the coracoid in *C. chilensis* (Fig. 2H). The origin of this muscle varies slightly in turtles, as in *Testudo* it arises from the lateral half of the coracoid and from the lateral fifth in *Emys* (Walker, 1973). The fleshy insertion of this muscle is broader in *P. hilarii* and in *H. tectifera*, filling the intertubercular fossa of the humerus; such insertion occurs on the ventral surface of the lateral process in *C. chilensis* (Fig. 3C,D). The *m. coracobrachialis brevis* is a minor retractor and adductor of the humerus and helps to strengthen the capsule of the shoulder joint (Walker, 1973).

Biceps complex. This complex is composed of *m. biceps superficialis* and *m. biceps profundus*. The biceps complex is variable in turtles (Walker, 1973; Yasukawa & Hikida, 1999), being formed either by two different muscles (superficialis and profundus, as observed in *P. hilarii* and *H. tectifera*) or by only one muscular mass (as in *C. chilensis*; Fig. 5B,C). This complex acts as a retractor of the humerus and a flexor of the antebrachium (Walker, 1973)*.*

Musculus biceps superficialis. This muscle has two equal bodies separated each other by an aponeurosis, just in the middle of its extension (in the middle of the humerus diaphysis). The proximal body arises as a fleshy attachment distal to the posterior edge of the coracoid (Figs 2G and 5B). The distal body arises from the aponeurosis and continues to insert by a short tendon at the ventral surface of the radius shaft as in *Trachemys* (Walker, 1973; Fig. 5D). This muscle is apparently absent in *C. chilensis.*

Musculus biceps profundus. Its fleshy attachment arises from the middle half and posterior edge of the coracoid, proximal to the glenoid fossa (Figs 2G and 5B). This muscle forms a tendon at the middle of the humeral diaphysis that inserts proximally into the ventral surface of the ulna and radius. This muscle inserts with the tendon of *m. brachialis inferior* (Fig. 5D). As stated above, in *C. chilensis* the entire biceps complex is represented by a single muscle that arises as a fleshy attachment from the ventral and posterior corner of the coracoid (Fig. 2H) and inserts through a tendon into the proximal third of the radius and ulna (Fig. 5C). This muscle is here interpreted as the *m. biceps profundus*.

Musculus brachialis inferior. This muscle has two heads in *P. hilarii* and in *H. tectifera* (Figs 3C and 5E), each one arising as fleshy attachment from the lateral and medial process of the humerus, contacting at the midshaft of the humerus and attaching by a tendon into the proximal third of the radius and ulna, at its facing edges. In *C. chilensis*, as in sea turtles (Walker, 1973), this muscle arises from the ventral surface of the midshaft of the humerus (Fig. 3D) and inserts as a fleshy attachment in the same region as in

P. hilarii and in *H. tectifera*. The *m. brachialis inferior* is a flexor of the antebrachium (Walker, 1973).

Extensors of the forelimb

Musculus extensor digitorum communis. This thin triangular sheet occupies the dorsal surface of the forelimb. In *P. hilarii* and in *H. tectifera*, as in *Podocnemis unifilis*, *Cuora amboinensis* and *Sacalia bealei* (Abdala et al. 2008), it arises by a tendon from the middle and dorsal surface of the distal epiphysis of the humerus (Fig. 3A) and extends reaching the digits (Walker, 1973; Abdala et al. 2008). This muscle is narrower in *P. hilarii* and in *H. tectifera* than in *C. chilensis* and it arises from the medial and dorsal surface of the radial epicondyle of the humerus (Fig. 3B). The origin surface of this muscle is the same in *C. chilensis* and in *Trachemys* (Walker, 1973). This muscle is an extensor of the feet and fingers (Walker, 1973).

Musculus tractor radii. This broad muscle occupies the medial side of the forelimb. In *P. hilarii* and *H. tectifera*, as in *Trachemys*, *Podocnemis unifilis*, *Cuora amboinensis* and *Sacalia bealei* (Walker, 1973; Abdala et al. 2008), it originates by a tendon on the transition surface between diaphysis and metaphysis, from the medial edge and slightly ventral surface of the humerus (Figs 3C and 5F). In *C. chilensis* the fleshy origin area is wider and extends to the ventral surface of the diaphysis of the humerus. In this species the *m. tractor radii* almost reaches the half shaft (Figs 3D and 5H). This muscle inserts as a fleshy attachment along the whole medial edge of the radius.

Musculus extensor radialis superficialis. This thin sheet goes along the *m. extensor digitorum communis* (Fig. 5F). It arises by a tendon from the dorsal surface of the distal epiphysis of the humerus, at the medial side of the origin of *m. extensor digitorum communis,* and inserts into the radiale (one of the bones of the autopodium). Whereas this muscle is clearly observed in *P. hilarii* and *H. tectifera* (Figs 3A and 5F), as in *Trachemys* (Walker, 1973), it is more difficult to differentiate in *C. chilensis,* since this muscle is joined to the *m. extensor radialis intermedius* (Fig. 5H). The join of these two muscles also occurs in *Carettochelys* and in some trionychids (Walker, 1973).

Musculus extensor radialis intermedius. This muscle extends at the medial side of *m. extensor radialis superficialis*. In *P. hilarii* and *H. tectifera* it arises by a tendon from the radial humerus epicondyle (Fig. 3A) and inserts fleshy throughout the medial edge of the radius, as opposed to *Trachemys* in which the *m. extensor radialis intermedius* inserts on the dorsal surface of the radius (Walker, 1973; Fig. 5F). In *C. chilensis* this muscle is joined to the *m. extensor radialis superficialis* sharing the origin and the insertion surface (Figs 3A and 5H).

Musculus extensor radialis profundus. This muscle lies deep to the *m. extensor digitorum communis*. It arises, by a tendon, deeper than the origin of *m. extensor radialis superficialis* (Fig. 5F) and it iserts fleshy along the dorsal surface of the radius, as opposed to *Trachemys* in which the *m. extensor radialis profundus* insert on the ulnar edge of the radius (Walker, 1973). In *C. chilensis* it is bulkier than in *P. hilarii* and *H. tectifera* (Fig. 5H).

The *m. tractor radii*, *m. extensor radialis superficialis*, *m. extensor radialis intermedius* and *m. radialis profundus* are all extensors of the radius (Walker, 1973).

Musculus extensor carpi ulnaris. As in other turtles (i.e. *Sacalia bealei* and *Cuora amboinensis;* Abdala et al. 2008), in the three species examined here, this muscle arises, by a tendon, from the lateral side of the origin of *m. extensor digitorum communis* and continues diagonally above the ulna to insert as a fleshy attachment in the laterodorsal surface of the ulna (Fig. 5F,H). This muscle is the only extensor acting on the ulnar side of the forelimb in *Trachemys* (Walker, 1973).

Musculus supinator manus. This triangular muscle lies under the *m. extensor digitorum communis* (Walker, 1973). In *P. hilarii* and *H. tectifera* it arises as a fleshy attachment from the proximal radial edge of the ulna and in *C. chilensis* as it arises fleshy from the distal end of the radial ulna edge (Fig. 5F,H). The origin of this muscle is different in *Trachemys*, since it arises from most of the radial side of the ulna (Walker, 1973). It inserts as a fleshy attachment upon the extensor surface of the first or second metacarpal. This muscle acts to supinate the feet (Walker, 1973).

Flexors of the forelimb

Musculus flexor carpi ulnaris. This muscle occupies all the lateral side of the forelimb. In *P. hilarii* and *H. tectifera,* as in other turtles such as *Podocnemis unifilis* and *Sacalia bealei* (Abdala et al. 2008), this muscle is divided in two branches (superficial and deep). The superficial branch arises, by a tendon, at the ulnar epicondyle of the humerus and inserts fleshy on the distal end of the ulna. The deep branch originates at the ulnar epicondyle of the humerus and it inserts along the lateral edge of the ulna (Fig. 3C). This muscle is divided in two branches in *C. chilensis* (medial and lateral), and the same happens in *Emys*, *Chelydra*, trionychids and *Carettochelys* (Walker, 1973). The medial branch arises, by a tendon, from the ulnar epicondyle of the humerus (Fig. 3D) and it inserts as a fleshy attachment on the distal end of the ulna. The lateral branch arises from the ulnar epicondyle of the humerus and it inserts along the lateral edge and part of the ventral surface of the ulna (Abdala et al. 2008). This muscle acts as a flexor of the forelimb and hand (Walker, 1973).

Musculus palmaris longus. In the three species studied here as in *Trachemys* (Walker, 1973), this muscle covers most of the ventral surface of the forelimb (Walker, 1973). It arises from a tendon in the ulnar epicondyle of the humerus (Walker, 1973), proximal to the origin of the *m. flexor carpi radialis* (Fig. 3C,D) and inserts into the flexor plate (Walker, 1973; Abdala et al. 2008; Fig. 5G).

Musculus flexor digitorum longus. This is a triangular muscle that lies deeper than the *m. palmaris longus*. As in other turtles, in the three species here studied it arises, by a tendon, from the ventral and medial surface at the proximal epiphysis of the ulna (Fig. 5G) and inserts into the flexor plate (Walker, 1973; Abdala et al. 2008).

The *m. palmaris longus* and *m. flexor digitorum longus* are important flexors of the forelimb, feet and digits (Walker, 1973).

Musculus flexor carpi radialis. In *P. hilarii* and *H. tectifera*, as in *Trachemys* (Walker, 1973), this muscle extends diagonally arising as a fleshy attachment from the ulnar epicondyle of the humerus at the medial side of the origin of the *m. palmaris longus*. In *C. chilensis,* however, it arises by a fleshy attachment from the medial edge of the humerus shaft. In the three species analyzed here, this muscle inserts on the distal condyle of the radius and on the first carpal (Walker, 1973; Abdala et al. 2008). The *m. flexor carpi radialis* is a flexor of the forelimb and feet (Walker, 1973).

Musculus pronator teres. As in other turtles (i.e. *Trachemys*; Walker, 1973), in the three specimens analyzed here, this muscle lies deeper than *m. flexor carpi radialis* and it goes in the same direction. It arises with a strong tendon attached to the ulnar epicondyle of the humerus between the origin of both *m. palmaris longus* and *m. flexor carpi radialis* and inserts fleshy at the ventral surface of the distal end of the radius (Fig. 5G). This muscle is a pronator of the forelimb and feet (Walker, 1973).

Musculus pronator profundus. In the three species analyzed, this muscle is triangular and is located deeper than the *m. flexor digitorum longus*. It arises, by a tendon, from the medial edge of the ulna at the distal side of the bicipital tubercle and inserts fleshy on the distal ulnar edge of the radius (Fig. 5G; Abdala et al. 2008).

Histological descriptions

The histological description is mostly focused on the presence, distribution, orientation and relative abundance of Sharpey's fibers and their possible relation with the previous analyzed muscular attachment of the pectoral girdle and humerus. Each thin section is described individually and according to its position on the pectoral girdle and humerus from proximal to distal.

For the histological description of the scapular girdle, we located the girdle in its anatomical posture and it was determined that the areas will be named as follows: the anterolateral will be the anterior, the anteromedial will be the medial, the posterolateral will be the lateral and, finally, the posteromedial will be the posterior.

The histological descriptions correspond to the following specimens: *C. chilensis* (AC), *P. hilarii* (MLPR 6402) and *H. tectifera* (MLPR 6411 and MLP R 6376).

Phrynops hilarii
Scapula
Scapular blade
The compacta is relatively narrower at the anterior and posterior areas of the cortex (Fig. 6A). Radially and longitudinally oriented vascular canals are seen at the medial area. The osteocyte lacunae are rounded in shape and disordered at the lateral and posterior areas. Their shape becomes mostly flattened at the outer cortex of the anterior area. Also, at the medial area, the lacunae are larger and their density increases. These lacunae are flattened and they are oriented perpendicular to the subperiosteal margin. Parallel-fibered bone predominates in the compacta. Sharpey's fibers are observed in relation to the *m. subscapularis* and *m. testocoracoideus* attachment site. These fibers are quite abundant in the lateral and medial areas, decreasing in density toward the anterior and posterior areas. At the lateral area, the Sharpey's fibers are clearly distinct. They form acute angles (40°) with respect to the subperiosteal margin at the posterolateral and anterolateral areas; and right angles at the lateral area (Fig. 6B). The same pattern is observed at the medial area. However, the density of Sharpey's fibers is increased in this area, providing a distinct mass birefringence to the bone tissue (Fig. 6C,D). At the anterior and posterior areas, Sharpey's fibers are located diagonally (16°–20° anteriorly; 39°–51° posteriorly).
Acromion
The medullary region, filled with trabecular tissue, is reduced. The cortex is narrower at the anterior and posterior areas. The compact bone is almost avascular. The osteocyte lacunae are mostly rounded; however, they are flattened at the outer cortex in the anterior area. The primary tissue is parallel-fibered bone. Sharpey's fibers are observed only in the dorsal and ventral areas. These fibers form acute angles (20°–80°) at the ventral area. At the dorsal area they exhibit a cross-pattern. Sharpey's fibers are located at the attachment site of *m. supracoracoideus anterior* (ventral and poster in part) and *m. deltoideus* (anterior and dorsal in part).
Coracoid
A wide medullary region, in relation to the cortical thickness, filled with trabecular tissue is seen. The cortical thickness is variable, being maximum at the dorsal (Fig. 6E) area and minimum at the ventral area. The cortex is poorly vascularized. The osteocyte lacunae have a rounded shape in
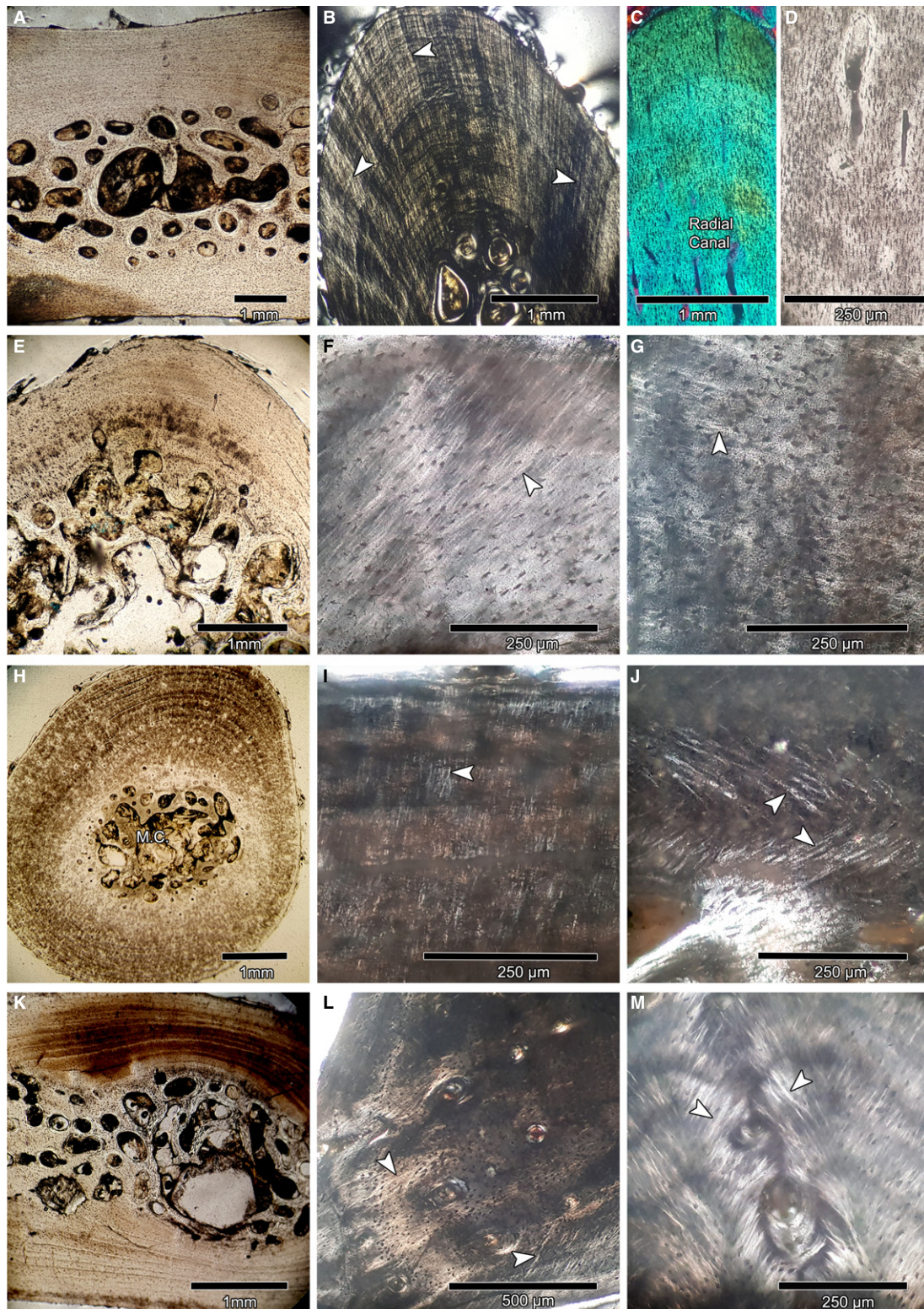
Fig. 6 Histological correlates of muscle attachment sites. (A–J) Thin slices of *Phrynops hilarii* (MLP R 6402): (A) anterior and posterior areas of the right scapular blade; (B) lateral area of the right scapular blade; (C,D) medial area of the right scapular blade; (E) dorsal area of the right coracoid; (F) anterior area of the right coracoid; (G) dorsal area of the right coracoid; (H) right humeral shaft; (I) ventral area of the right humeral shaft; (J) dorsal area of the right distal metaphysis of the humerus; (K–M) thin sections of *H. tectifera* (MLPR 6376): (K) anterior and posterior area of the left scapular blade; (L) medial area of the left scapular blade; (M) lateral area of the left scapular blade; M.R, medular region. Arrows = Sharpey's fibers. (A,D,E,H,K) are under normal light; (B,F,G,I,J,L,M) are under polarized light; (C) is under polarized light with lambda compensator.

the dorsal and anterior areas and are flattened in the posterior and ventral areas. The microstructure of the tissue allows it to be recognized as parallel-fibered bone. Sharpey's fibers can be distinguished in the whole compacta. At the posterior and anterior areas, these fibers are abundant and obliquely (50°–60° anteriorly and 33°–42° posteriorly) oriented with respect to the subperiosteal margin (Fig. 6F). Sharpey's fiber density tends to decrease towards the dorsal and ventral areas. These fibers are in acute angles with respect to the subperiosteal margin at the dorsal (75°–90°) and ventral (38°–60°) areas (Fig. 6G). All these fibers are at the attachment site of *m. coracohyoideus* (anterodorsal), *m. coracobrachialis magnum* (dorsal), *m. coracobrachialis brevis* (posterodorsal), *m. biceps profundus* (posterior) and *m. supracoracoideus posterior* (anterior and ventral).

Humerus

Proximal metaphysis

The bone wall is thin and encloses a large medullary region filled with bony trabeculae. The cortical thickness is roughly the same throughout the circumference. Vascular spaces are almost absent, although there are some longitudinal canals in the inner cortex at the ventral area. Whereas the osteocyte lacunae are rounded and disordered at the dorsal area, they are flattened and organized at the ventral area. The density of the osteocyte lacunae is particularly increased at the medial and ventromedial areas. These lacunae do not exhibit any predominant shape or arrangement in this area. Parallel-fibered bone matrix is recognized as the main component of the cortex at the ventral area. Abundant Sharpey's fibers are observed at the whole dorsal area (i.e. *m. latissimus dorsi* + *m. teres major*, *m. deltoideus* and *m. subscapularis* attachment sites). These fibers are mostly oriented at a right angle with respect to subperiosteal margin. Sharpey's fibers are distinct at the dorsomedial, medial and ventromedial areas (attachment site of *m. triceps brachii* and *m. pectoralis*). These fibers are located in a cross-pattern with respect to subperiosteal margin.

Diaphysis

This consists of a thick cortex surrounding a narrow medullary region filled with bony trabeculae (Fig. 6H). The cortical thickness decreases at the dorsal area. Longitudinal vascular canals are only observed at the lateral area. The osteocyte lacunae are flattened at the outer cortex and slightly rounded in the inner core. Such pattern varies at the dorsolateral area, where osteocyte lacunae are flattened in both inner and outer cortex. The main component of the cortex is lamellar bone. Sharpey's fibers are only observed at the ventral area. These fibers are perpendicular and at acute angles (65°–90°) with respect to the subperiosteal margin and they are located at the *m. brachialis inferior* attachment site (Fig. 6I).

Distal metaphysis

The bone wall is thin and encloses a large medullary region filled with bony trabeculae. The cortical thickness

decreases at the lateral and medial area. The cortex is avascular. The osteocyte lacunae are mostly rounded throughout the cortex. Sharpey's fibers are more abundant at the dorsal area, at the *m. triceps brachi* attachment site. These fibers exhibit two main orientations (cross-pattern). Whereas a group of fibers is oriented toward the lateral side, forming an angle of 44° with the surface of the bone, others are projected toward the medial side, forming an angle of 40°. It is worth noting that the former is more abundant at the outer cortex and the latter at the perimedullary cortex (Fig. 6J). Sharpey's fibers are located diagonally (33°–49°) from the subperiosteal margin and cross the entire cortex at the lateral area. They are more evident at the *m. palmaris longus* or *m. flexor carpi radialis* attachment sites.

Hydromedusa tectifera

Scapula

Scapular blade

The cross-section has a reduced medullary region. The cortical thickness is not uniform, being slightly narrower in the anterior and posterior areas (Fig. 6K). Rows of longitudinally oriented vascular canals are located from the medullary region to the outer cortex at the lateral and medial areas. Poorly organized osteocyte lacunae of rounded shape are observed at the medial, lateral and anterior areas. Osteocyte lacunae are denser at the medial and lateral areas. Such an increased density of lacunae coincides with the regions in which vascular canals are present. At the posterior area, osteocyte lacunae exhibit variable shapes (i.e. from flattened to rounded) at the posterior region. Parallel-fibered bone matrix is recognized as the main component of the cortex. Sharpey's fibers are observed in different orientations and densities around the scapular blade, at *m. testocoracoideus* and *m. subscapularis* attachment site. These fibers show both perpendicular and acute angles (cross-pattern) with respect to the subperiosteal margin at the medial area (Fig. 6L). In the posterior area, particularly at the posteromedial area, the fibers are spaced apart and oriented at right and acute angles (75°–90°). On the other hand, at the posterolateral area, the fibers are more densely grouped and are oriented diagonally (36°–46°) with respect to the subperiosteal margin. Sharpey's fibers are observed in two main directions in the lateral area, forming a cross-pattern (Petermann & Sander, 2013; Figs 6M and 7A). This pattern is clearly seen in the region where the vascular canals are located. In the anterior area, particularly at the anteromedial and anterolateral region, the extrinsic fibers are abundant and diagonally oriented (30°–51°). Conversely, their density decreases in the anterolateral area, where they are at acute angles (57°–85°) with respect to the subperiosteal margin.

Acromion

This section presents a wide medullary region formed by trabecular tissue. The cortex is narrower in the anterior and

posterior areas (Fig. 7B). Vascularization is only observed in the dorsal and ventral areas. The dorsal area presents a row of longitudinal vascular canals arranged radially, extending from the medullary region to the outer cortex. In the ventral area, there are several rows of longitudinal vascular canals which are located from the medullary region to the outer cortex. The osteocyte lacunae have a rounded shape throughout the cortex. Sharpey's fibers are observed throughout almost the whole cortex. The density of extrinsic fibers is higher at the dorsal and ventral areas. Also, in these areas, the fibers are in cross-pattern (Petermann & Sander, 2013; Fig. 7C). In the posterior area, the fibers are located at acute (49°–70°) and right angles with respect to the subperiosteal margin. Sharpey's fiber density decreases toward the anterior area. These fibers are mostly in a right angle with respect to the subperiosteal margin. Sharpey's fibers correspond with the attachment site of *m. deltoideus* (anterior, ventral and dorsal) and *m. supracoracoideus anterior* (ventral, posteriorly and dorsal).

Coracoid

The cross-section is composed of a small medullary region surrounded by a cortex, which is thicker in the posterior area (Fig. 7D). Few longitudinal and radial vascular canals are observed. The osteocyte lacunae are rounded in shape. Their density is higher at the ventral area, where they are strongly disorganized. At the dorsal area the osteocyte lacunae are mostly flattened. Parallel-fibered bone matrix is recognized as the main component of the cortex. Sharpey's fibers with variable orientations are observed at the posterior portion of the cortex. The extrinsic fiber density decreases from posterodorsal to posteroventral area. Their orientations varied from oblique (45°) to perpendicular (90°) with respect to the subperiosteal margin (Fig. 7E). Less densely grouped Sharpey's fibers are observed at the anterior area, where they are arranged perpendicular to the outer surface. Sharpey's fibers located at the ventral area exhibit more than two orientations (Fig. 7F). These extrinsic fibers correspond with the attachment site of *m. coracobrachialis magnus* (dorsally), *m. coracobrachialis brevis* (posterodorsally), *m. biceps profundus* (posteriorly) and *m. supracoracoideus posterior* (anteriorly and ventrally).

Humerus

Proximal metaphysis

The cortical bone is thicker at the dorsal and ventral areas, becoming narrower toward the medial and lateral areas. The cortical thickness decreases considerably at the dorsomedial area. Some longitudinal and radial vascular canals are observed at the ventral area. Osteocyte lacunae are flattened at the outer cortex of the dorsal area. However, they are mostly rounded and denser in the other parts of the cortex. Also, the density of osteocyte lacunae increases at the medial area. At the inner core of the ventral area, the osteocyte lacunae are mostly rounded in shape and more densely grouped; at the outer cortex they become mostly flattened in shape. The cortex consists of parallel-fibered/lamellar bone. Sharpey's fibers located at the dorsally half of the cortex exhibit three different patterns. These fibers are inserted at the dorsolateral area, forming an angle of approximately 50°–67° to the surface. At the dorsal area, the cortex is full of fibers which penetrate the cortex at an angle of 51°–70° (Fig. 7G,H). Some flattened osteocyte lacunae are oriented in the same direction as the Sharpey's fibers in this region. These patterns of fiber orientation are found at the attachment site of *m. latissimus dorsi + m. teres major*, *m. deltoideus* and *m. subscapularis*. At the dorsomedial and medial area, the *m. triceps brachii* and *m. pectoralis* attachment site is characterized by the presence of abundant Sharpey's fibers. These fibers are located at right angles with respect to the subperiosteal edge.

Diaphysis

The cortex has a variable thickness, being narrower in the dorsal area. The medullary region is filled with cancellous bone with a few bony trabeculae (Fig. 7I). The cortex is almost avascular, with some vascular spaces located at the medial area. The osteocyte lacunae are more abundant at the subperiosteal margin than at the perimedullary cortex. These lacunae exhibit a rounded appearance in almost all the cortex, but they become flattened at the outer cortex of the lateral and medial regions. Parallel-fibered/lamellar bone tissue is the main component of the cortex. Sharpey's fibers are recognized in both dorsal and ventral areas (i.e. *m. brachialis inferior* and *m. triceps brachii* attachment areas; Fig. 7J), being more abundant at the ventral area. These fibers are oriented at acute (60°) and right angles to the subperiosteal margin.

Distal epiphysis

The cortical thickness is roughly the same in the whole element, except in the ventral area, where it becomes thinner. With the exception of the ventral area, there are some longitudinal vascular canals. Osteocyte lacunae at the dorsal area are disorganized and they exhibit a rounded appearance at the outermost cortex. On the other hand, osteocyte lacunae at the inner cortex are flattened and well organized, forming two distinct 'layers'. One of these layers is located outside the resorption line. The density of the osteocyte lacunae increases at the dorsolateral area in comparison with the ventral and medial area. In these three areas, the lacunae lack a particular arrangement. At the dorsal and dorsolateral area, Sharpey's fibers are abundant at the *m. triceps brachii* attachment site. These fibers are located diagonally (20°–47°) and are observed from the outer cortex of the lateral area to the medullar region (Fig. 7K).

Chelonoidis chilensis
Scapula
Scapular blade

The material exhibits a wide medullary region surrounded by the cortex. The latter has a variable thickness, being narrow in the lateral, anterior and posterior areas
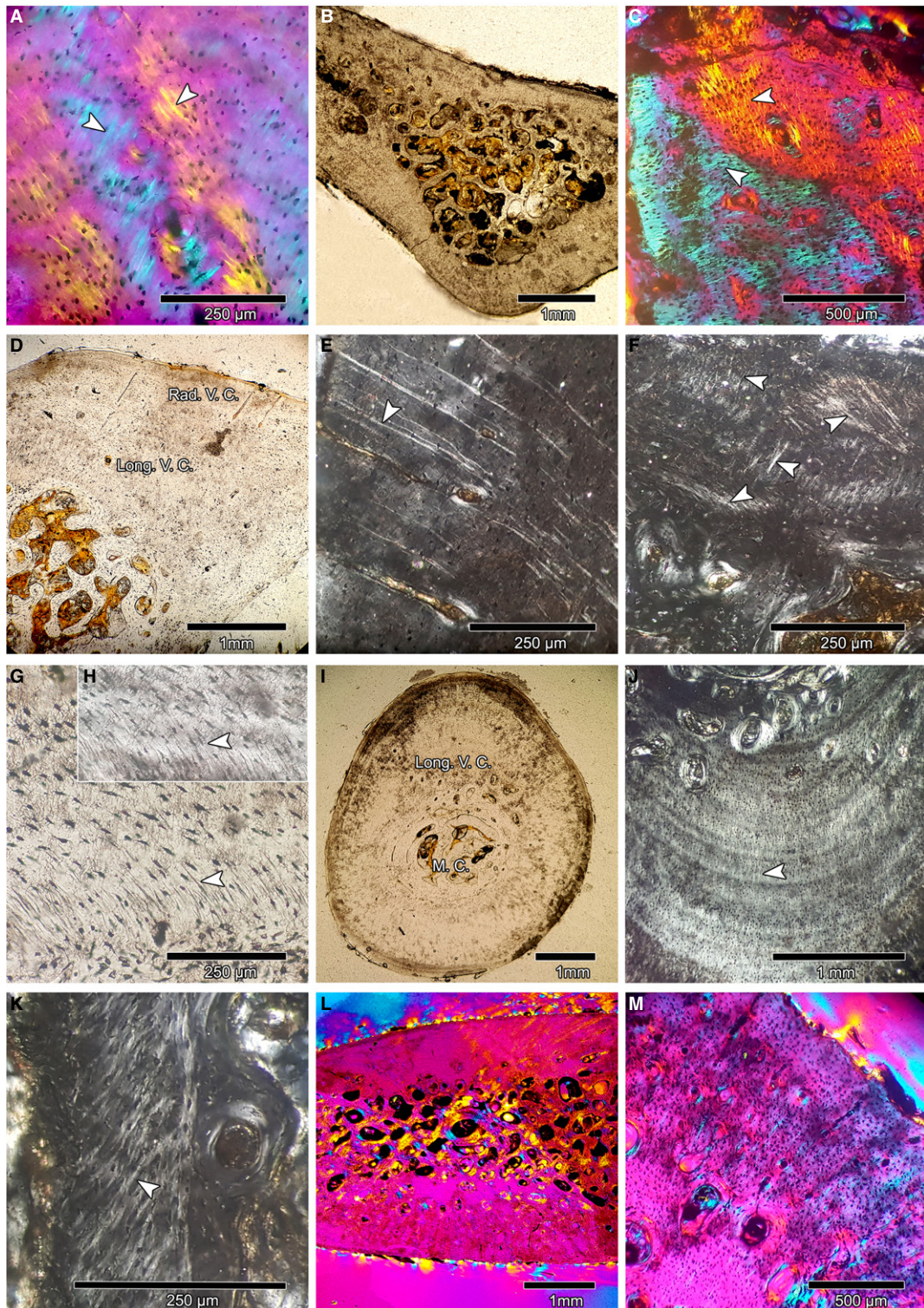
Fig. 7 Histological correlates of muscle attachment sites. (A–C) Thin sections of *Hydromedusa tectifera* (MLPR 6376) and (D–K) thin sections of *H. tectifera* (MLPR 6411): (A) lateral area of the left scapular blade; (B) left acromion; (C) ventral area of the left acromion; (D) right coracoid; (E) posterior area of the right coracoid; (F) ventral area of the right coracoid; (G,H) dorsal area of the proximal metaphysis of the right humerus; (I) diaphysis of the right humerus; (J) ventral area of the diaphysis of the right humerus; (K) dorsal area of the distal metaphysis of the right humerus. (L,M) Thin sections of *Chelonoidis chilensis* (AC): (L) anterior and posterior area of the right scapular blade; (M) anterior area of the right scapular blade. Long.V.C, longitudinal vascular canals; Rad.V.C, radial vascular canals. Arrows = Sharpey's fibers. (B,D,G,I) are under normal light; (E,F,H,J,K,M) are under polarized light; (A,C,L,M) is under polarized light with lambda compensator.

(Fig. 7L). Vascularization is observed in the medial, lateral and anterior areas. There is a higher density of vascular canals in the anterior area. The vascular canals are mostly oriented longitudinally, although some radial canals are also present (Fig. 7M). The osteocyte lacunae have a rounded shape and do not present an organized pattern. Their shape becomes more flattened in the posterolateral area of the outer cortex. The osteocyte lacunae are more closely arranged in the anterior area than in the posterior and medial areas. Osteocyte lacunae are relatively larger and more densely arranged in the lateral cortex than in the other portions of the compacta. Primary bone tissue consists of parallel-fibered bone, with fibers oriented parallel to the axis of the element. Around the cortex of the scapular blade (attachment site of *m. deltoideus* and *m. subscapularis*) the Sharpey's fibers observed are in different patterns. Their density is more pronounced in the medial area, where they exhibit a cross-pattern (Petermann & Sander, 2013). Fibers with more than two orientations are observed in the anterolateral and lateral areas (Fig. 8A). However, there is a lower density of fibers in the anterior area, in which they are at acute and right angles (63°–80°) with respect to the subperiosteal margin (Fig. 8B). A higher density of fibers is observed at the posterior area, particularly at the posteromedial region. These fibers are located diagonally (27°–46°) to the subperiosteal margin (Fig. 8C).

Acromion

In the cross-section, a wide medullary region filled with spongy tissue is observed. The thickness of the cortex varies, it being narrower in the anterior area than in the rest of the areas. The cortex is well vascularized, mainly presenting longitudinal canals. The osteocyte lacunae have a rounded shape and are randomly arranged, except in the posteroventral area, where some lacunae are flattened in shape and the lacunae are closer to each other. Particularly the flattened osteocyte lacunae are oriented transversal to the subperiosteal margin (Fig. 8D). The cortex is formed by parallel-fibered bone. Abundant Sharpey's fibers are observed throughout the whole acromion cortex. At the dorsal, anterior and posterior areas (i.e. attachment site of *m. deltoideus* and *m. subscapularis*), fibers are observed continuously. These fibers have an oblique orientation (60°–40°) with regard to the subperiosteal margin at the anterior and posterior areas, becoming perpendicular at the dorsal area. Ventrally, at the *m. supracoracoideus anterior* attachment site, a different pattern of Sharpey's fibers is observed. At the posteroventral area the fibers are

located in acute angle and then continue roughly concentrically (i.e. almost reaching the subperiosteal margin; Fig. 8E); at the ventral area, the fibers are located diagonally to the subperiosteal margin (26°–33°).

Coracoid

The cortical thickness varies, being wider in the ventral area than in the rest of the cortex (Fig. 8F). There are a few longitudinal vascular canals. The osteocyte lacunae have a rounded shape and they exhibit a disorganized pattern. The matrix corresponds to parallel-fibered bone. Sharpey's fibers are observed throughout the ventral area, at the attachment site of *m. supracoracoideus posterior*. These fibers decrease in density from the anterior to the posterior area. Also, its orientation changes, being oblique (62°) with respect to the subperiosteal margin in the anteroventral area (Fig. 8G) to perpendicular with respect to the subperiosteal margin in the ventral (Fig. 8H) and posteroventral areas (Fig. 8I). At the posterior area (i.e. *m. coracobrachialis brevis* attachment site) abundant fibers are located diagonally (46°–65°) to the subperiosteal margin. Their orientation is the same at the posterodorsal area, but they are less abundant. Finally, at the dorsal area (i.e. *m. coracobrachialis magnus* attachment site) a few short fibers with more than two orientations are observed.

Humerus

Proximal metaphysis

The thickness of the cortex varies in its circumference, being wider at the dorsal area. The medullary region is filled by abundant bony trabeculae. The cortex is almost avascular, with some longitudinal vascular canals at the dorsal and ventral areas. The osteocyte lacunae have different shapes, arrangements and densities around the cortex. At the dorsolateral area, they are rounded and well organized with each other. Also at this area, but close to the lateral area, osteocyte lacunae are randomly arranged and present a high density. At the ventrolateral area, the osteocyte lacunae are flattened and organized. At the ventral area, the lacunae are mostly flattened and disorganized. At the dorsolateral and ventral areas, parallel-fibered bone is observed at the outer cortex. The perimedullary cortex is composed of compacted coarse-cancellous bone. This tissue is well developed and almost reaches the outer cortex at the medial and lateral areas. At the dorsal area (from medial to lateral area), Sharpey's fibers exhibit different densities and orientations depending on the different muscle attachment sites. At the attachment site of *m. deltoideus*, Sharpey's fibers are

Fig. 8 Histological correlates of muscle attachment sites. (A–L) Thin sections of *Chelonoidis chilensis* (AC): (A) anterolateral area of the right scapular blade; (B) anterior area of the right scapular blade; (C) posteromedial area of the right scapular blade; (D) posterior area of the right acromion; (E) ventral area of the right acromion; (F) right coracoid; (G) anteroventral area of the right coracoid; (H) ventral area of the right coracoid; (I) posteroventral area of the right coracoid; (J) dorsal area of the right proximal metaphysis of the humerus; (K) diaphysis of the right humerus; (L) ventral area of the diaphysis of the right humerus. Arrows = Sharpey's fibers. (K) is under normal light; (A–C,E–J) is under polarized light; (D,L) are under polarized light with lambda compensator.
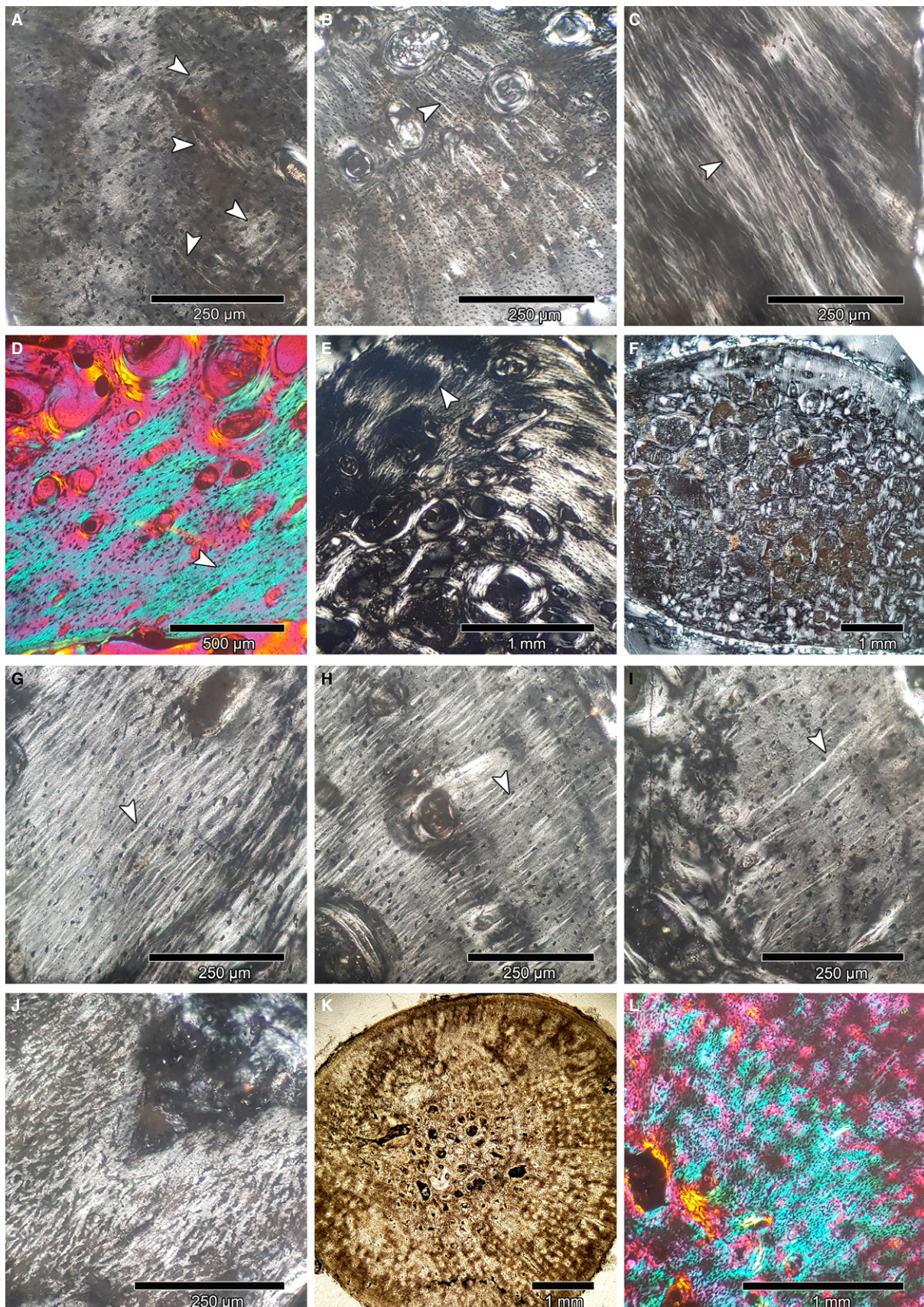
arranged diagonally (40°–67°) with respect to the subperiosteal margin and sub-parallel to the bone axis. Their density in this area is relatively lower in comparison with other areas. A higher density of these fibers is observed at the attachment site of *m. latissimus dorsi* + *m. teres major*, where they are arranged in right angles to the subperiosteal margin. In this region, abundant flattened osteocyte lacunae are oriented in the same direction as the Sharpey's fibers (Fig. 8J). A low density of Sharpey's fibers is observed at the attachment site of *m. subscapularis*, where they are oriented diagonally (26°–49°) with respect to the subperiosteal edge. At the ventral area, Sharpey's fibers are observed at the *m. pectoralis* attachment site. These fibers are diagonally (25°–38°) arranged. Sharpey's fibers at the lateral area are arranged diagonally (52°–72°) with respect to the subperiosteal margin.

Diaphysis

The diaphysis consists of a thick cortex surrounding a narrow medullary region filled with bony trabeculae. The cortex becomes thinner at the dorsal area (Fig. 8K). The compacta is vascularized with several longitudinal and radial vascular canals. This vascularization tends to decrease toward the outermost cortex. In the dorsal area, at the inner cortex, the osteocyte lacunae are rounded and randomly arranged. The osteocyte lacunae are flattened in shape and more spatially ordered at the medial and lateral areas of the cortex. These lacunae become more flattened at the subperiosteal region. At the ventral area, the osteocyte lacunae exhibit variable shapes and arrangements, being rounded and disordered in some areas or flattened and well organized (i.e. oriented perpendicular to the subperiosteal margin) in others. In the areas where Sharpey's fibers are seen, the osteocyte lacunae are flattened. At the ventral area, Sharpey's fibers are oriented from the medullary region to the outer cortex at right angles (Fig. 8L). These fibers are at the attachment site of *m. brachialis inferior*. At the dorsal, ventral, lateral and medial areas, a thin 'layer' of Sharpey's fibers at the outer cortex are observed. These fibers penetrate the cortex (44°) diagonally and are at the attachment site of *m. triceps brachii*.

Distal metaphysis

The distal metaphysis consists of a thick cortex surrounding a large medullary region that contains bony trabeculae. There are a few longitudinal vascular canals at the dorsal and lateral areas of the cortex. These spaces become more abundant at the inner cortex of the dorsal region. The osteocyte lacunae have different shapes, arrangements and densities in different areas of the cortex. At the dorsal area, they are slightly rounded and disordered. In the dorsomedial area, there is a thin 'layer' where the lacunae are flattened and organized. The same pattern is also observed at the ventromedial area. Finally, at the medial area, there are small regions in which these structures are dense and randomly arranged. The main tissue at the dorsomedial area, which consists of lamellar bone, has been almost entirely eroded by osteoclastic activity and cortical bone is mostly composed of compacted coarse-cancellous bone. This bone tissue is also observed at the medial, ventral and lateral areas of the cortex. Abundant Sharpey's fibers are observed at the dorsal area, which penetrate the cortex diagonally (30°–68°) from the subperiosteal edge at the medial area and extend toward the inner core. These extrinsic fibers are located at the *m. triceps brachii* attachment site. A thin 'layer' of Sharpey's fibers is recognized at the outer cortex of the ventral area, specifically at the area of the *m. brachialis inferior* attachment site. These fibers penetrate the cortex at right angle.

As a result of the histological observations, different patterns related to the orientation and distribution of Sharpey's fibers were determined and are summarized in Table 2.

Orientation patterns: Type I: parallel fibers: at right or acute angles with respect to the subperiosteal margin (e.g. attachment site of *m. subscapularis* in the acromion of *C. chilensis,* Figs 8D and 9); Type II: fibers in an organized cross-pattern, forming angles between them in two main orientations (at acute and right angles or two acute angles, e.g. attachment site of *m. subscapularis* in *H. tectifera*; Figs 7A and 9) and Type III (Fig. 9): fibers in a disorganized cross-pattern, arranged at more than two orientations (e.g. attachment site of *m. supracoracoideus posterior* in *H. tectifera*; Fig. 7F).

Distribution patterns: Type A: fibers spaced apart (e.g. attachment site of *m. subscapularis* in *C. chilensis;* Fig. 8B); Type B: fibers are densely grouped but it is still possible to differentiate one from each other (e.g. attachment site of *m. supracoracoideus posterior* in *P. hilarii*, Fig. 6F); Type C: fibers are so densely grouped that it is not possible to differentiate one from each other (e.g. attachment site of *m. latissimus dorsi* + *m. teres major* in *C. chilensis*; Fig. 8J, and the attachment site of *m. testocoracoideus* in *P. hilarii*; Fig. 6C,D).

Discussion

Myological analysis

Turtles perform aquatic and terrestrial locomotion. Particularly, aquatic, marine and freshwater turtles also spend part of their lives in the terrestrial environment, although the marine ones spend less time on land (Bennett et al. 1970; Zug, 1971; Davenport et al. 1984). With respect to the locomotor skills of turtles, marine turtles are better swimmers than walkers, freshwater turtles have great locomotor skills in both water and on land, and terrestrial tortoises are agile on land and do not swim (Davenport et al. 1984). In general, while swimming, the muscles propel the body against the water (Depecker et al. 2006), overcoming the resistance of water. Therefore, the muscles that act during aquatic locomotion are protractors (Rivera & Blob, 2010). During

Table 2 Correlation between muscle attachments and Sharpey's fiber orientation and distribution.

Skeletal element	Muscle attachment	*Phrynops hilarii*	*Hydromedusa tectifera*	*Chelonoidis chilensis*
Scapular blade	In. *Tstocor.*	SF continuous Type I Type C	SF continuous Type II Type B	–
	Or. *Sbscap.*	SF in patches Type I Type B	SF in patches Type I, II Type B	SF in patches Type I, III Type A, B
	Or. *Dl. Scap.*	–	–	SF continuous Type II Type B
Acromion	Or. *Dl. Clav.*	SF in patches Type II Type B	SF in patches Type I, II Type B	SF continuous Type I Type B
	Or. *Sbscap.*	–	–	SF continuous Type I Type B
	Or. *Spcor, Ant.*	SF in patches Type I Type B	SF in patches Type II Type B	SF continuous Type I Type B
Coracoid	Or. *Spcor, Post.*	SF in patches Type I Type B	SF continuous Type I, III Type B	SF continuous Type I, A Type B
	In. *Corhy.*	SF continuous Type I Type B	–	–
	Or. *Corbra. M.*	SF continuous Type I Type B	SF in patch. Type I Type B	SF continuous Type I Type B
	Or. *Corbra. B.*	SF continuous Type I Type B	SF continuous Type I Type B	SF continuous Type III Type B
	Or. *Bic. Pro.*	SF in patch. Type I Type B	SF continuous Type I Type A	–
Humerus - Proximal metaphysis	In. *Lat. D. & Ter. Mj.*	SF continuous Type I Type B	SF continuous Type I Type B	SF continuous Type I Type C
	In. *Dl.*	SF continuous Type I Type B	SF continuous Type I Type B	SF continuous Type II Type B
	In. *Sbscap.*	SF continuous Type I Type B	SF continuous Type I Type B	SF continuous Type I Type B
	Or. *Tri.*	SF continuous Type II Type B	SF continuous Type I Type B	–
	In. *Pect.*	SF continuous Type II Type B	SF continuous Type I Type B	SF continuous Type I Type B
Humerus - Diaphysis	Or. *Brac.*	SF continuous Type I Type B	SF continuous Type I Type B	SF continuous Type I Type C
	Or. *Tri.*	–	SF continuous Type I Type B	SF continuous Type I Type B

(continued)

Table 2 *(continued)*

Skeletal element	Muscle attachment	*Phrynops hilarii*	*Hydromedusa tectifera*	*Chelonoidis chilensis*
Humerus - Distal metaphysis	Or. *Tri.*	SF continuous Type II Type B	SF continuous Type I Type B	SF continuous Type I Type B
	Or. *Brac.*	–	–	SF continuous Type I Type B
	Or. *Pal. L.* or Or. *Flex. C. R.*	SF continuous Type I Type B	–	–

Bic. Pro., biceps profundus; Brac., brachialis inferior; Dl., deltoideus; Dl. Clav., deltoideus claviculari; Dl. Scap., deltoideus scapularis; Corbra. B., coracobrachialis brevis; Corbra. M., coracobrachialis magnus; Corhy., coracohyoideus; Flex. C. R., flexor carpi radialis; In., insertion; Lat. D. & Ter. Mj., latissimus dorsi and teres major; Pal. L., palmaris longus; Or., origin; Pect. Pectoralis; Sbscap., subscapularis; SF., Sharpey's fibers; Spcor. Ant., supracoracoideus anterior; Spcor. Post., supracoracoideus posterior; Tri., triceps brachii; Tstocor., testocoracoideus. In the classification of Type I, the Sharpey's fibers are parallel to each other and in acute or right angles to the subperiosteal margin. In Type II, the Sharpey's fibers form an angle to each other in two main orientations. In Type III, the Sharpey's fibers form an angle to each other in more than two orientations. Type A, the Sharpey's fibers are apart from each other. Type B, the Sharpey's fibers are densely grouped but it is still possible to differentiate one from each other. Type C, the Sharpey's fibers are densely grouped, so it is not possible to distinguish one from each other.

terrestrial locomotion, the muscles must offer support as well as propulsion (Depecker et al. 2006). In this type of locomotion, the retractor muscles exert vertical force to support the weight of the body against the force of gravity (Jayes & Alexander, 1980; Rivera & Blob, 2010).

As a result of our analysis, and as has been pointed out in other studies (Walker, 1971, 1973; Yasukawa & Hikida, 1999; Abdala et al. 2008; Rivera & Blob, 2013), we found differences in the forelimb musculature between the aquatic and terrestrial turtles (*P. hilarii* – *H. tectifera* and *C. chilensis*, respectively) in the muscles involved in the movements of the stylopodium and zeugopodium. Some of these were not previously reported and they are related to the insertion of the *m. pectoralis*, the *m. coracobrachialis magnus* and the origin of the *m. tractor radii*. All the differences correspond to the size and shape of some muscle attachment sites and the fusion of muscles. In *C. chilensis* the *m. extensor radialis superficialis* is joined with the *m. extensor radialis intermedius* (both extensors of the radius), and the *biceps complex* (retractor of the humerus and flexor of the zeugopodium) is composed of a single muscle. The *m. biceps superficialis* and *m. biceps profundus* are independent muscles in *P. hilarii* and *H. tectifera*, as occur in other Testudines such as *Trachemys*, *Chelydra*, trionychids, *Carettochelys*, *Pelomedusa* and *Chelodina* (Walker, 1973; Yasukawa & Hikida, 1999). As in *C. chilensis*, a variation of this condition is present in other testudinids and sea turtles (e.g. *Testudo* and *Dermochelys*), where the entire biceps complex is represented by a single muscle (or by only one muscle partially separated; Walker, 1973). Some authors have shown that the biceps could develop as a single mass and separate in superficial and deep parts in late ontogeny (e.g. *Chrysemys* Walker, 1973). The functional value of a single or double *m. biceps* in turtles has not been evaluated, but the configuration (single biceps) present in sea turtles has been mentioned as an adaptation for a compact, streamlined fin (Walker, 1973).

In these two groups of turtles (aquatic and terrestrial), the attachment sites of some muscles are more extended in *C. chilensis*. These muscles are: the *m. deltoideus* (abductor and protractor of the humerus, and rotator of the entire pectoral girdle during the limb protraction), *m. pectoralis* (retractor and adductor of the humerus), *m. subscapularis* (abductor of the arm and protractor of the limb) and *m. tractor radii* (extensor of the radius). Rotation of the pectoral girdle allows the humerus to rotate on its longitudinal axis, rising and lowering the limb; the adductor muscles are also needed to keep the humerus horizontal when the feet are on the ground (Walker, 1971). In contrast, the attachment sites of the *m. supracoracoideus anterior* (adductor and retractor of the humerus), *m. coracobrachialis magnus* (retractor of the humerus) and *m. brachialis inferior* (flexor of the antebrachium) are smaller in *C. chilensis* than in *P. hilarii* and *H. tectifera*. The relatively largest attachment sites of retractor and flexor muscles in aquatic turtles allow the humerus to be strongly retracted and the forearm to be flexed with considerable force, so the limb can be pulled far forward at the beginning of a propulsive stroke (Walker, 1973).

In relation to the autopodium muscles, some differences between freshwater and terrestrial turtles were observed. The tendon of the *m. extensor digitorum communis* (extensor of the digits) is more pronounced in *C. chilensis* than in *P. hilarii* or *H. tectifera*. Abdala et al. (2008) pointed out
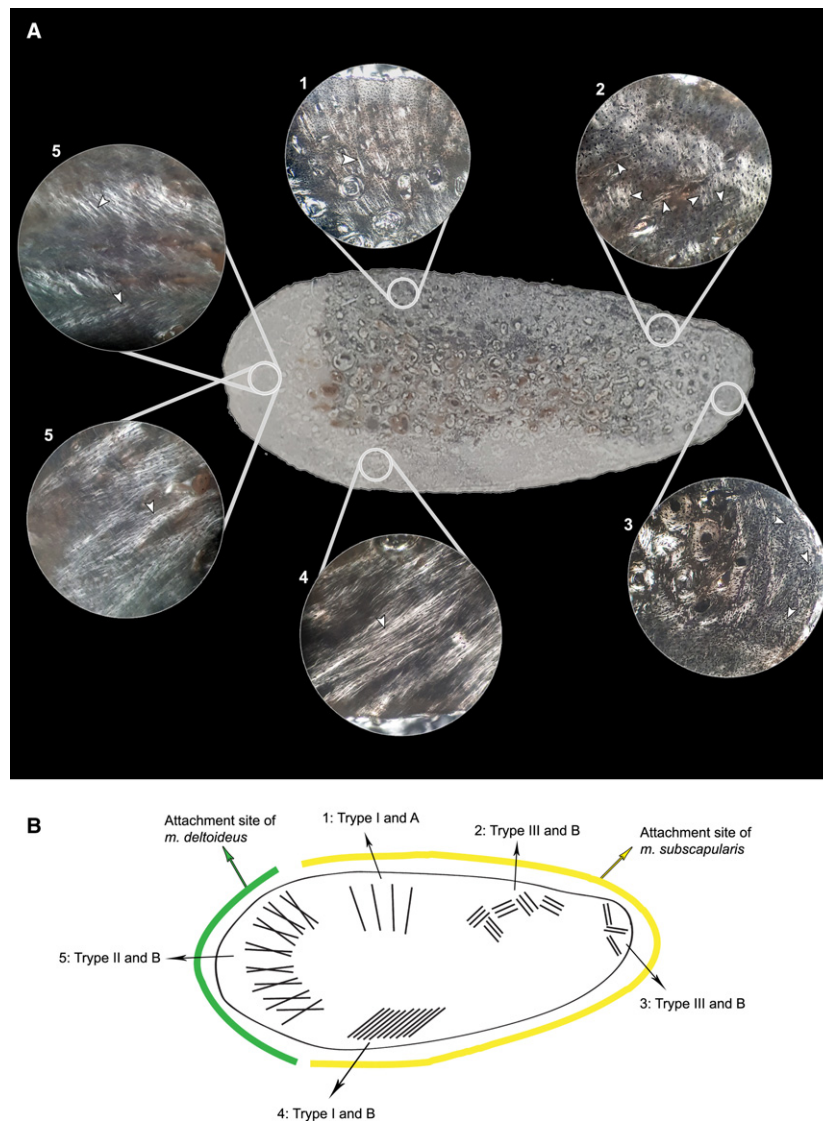
Fig. 9 Picture (A) and schematic drawing (B) of *m. subscapularis* attachment sites and the SF (Sharpey's fibers) in the *Chelonoidis chilensis* scapular blade. With special attention to the different types of orientation and density of Sharpey's fibers. Arrows = Sharpey's fibers. All the pictures are under polarized light.

that the extensor muscles of the distal forelimb are heavier in terrestrial turtles, providing more body support and propulsion. The *m. flexor carpi radialis* (flexor of the zeugo and autopodium) has a different origin in both groups of turtles, arising from the humerus diaphysis in *C. chilensis* and from the ulnar epicondyle in *P. hilarii* and *H. tectifera*.

Despite some of these specific differences, the general morphology of the limb musculature in turtles is almost the same in all the species (Walker, 1973; Abdala et al. 2008). However, muscles such as *m. supracoracoideus anterior*, *m. subscapularis*, *m. coracobrachialis magnus*, *m. coracobrachialis brevis*, *m. extensor radialis intermedius*, *m. pectoralis* and *m. tractor radii* have different features in aquatic and terrestrial turtles in relation to the extent of

their attachment surface, a variation that could be related to different locomotion habits.

Sharpey's fibers in the muscle attachment site

Sharpey's fibers were observed in almost all the muscle attachment sites, both fleshy and tendinous, but did not extend through the whole surface of the sites. Therefore, the boundaries of a muscle attachment area cannot be determined by the presence of Sharpey's fibers (Hieronymus, 2006; Petermann & Sander, 2013). In several thin sections, we observed the concentration of Sharpey's fibers only in a region of total extension of the muscular attachment. This pattern could be related to what was proposed

by Suzuki et al. (2002) and Petermann & Sander (2013), who stated that the region where these extrinsic fibers are observed is the place where the muscle exerts the force. From all the attachment sites analyzed (13 muscles), Sharpey's fibers were only distributed in patches at the origin of four muscles (*m. subscapularis*, *m. supracoracoideus anterior* and *posterior*, *m. deltoideus* and *m. biceps profundus*). The patchy distribution of *m. subscapularis* was recorded in all three taxa analyzed. In the case of the *m. supracoracoideus anterior* and *m. deltoideus*, their limited distribution (i.e. patchy) was observed only for *H. tectifera* and *P. hilarii*; however, the distribution of the fibers is reduced in *P. hilarii* compared with *H. tectifera*. Finally, the patchy distribution of *m. supracoracoideus posterior* and *m. biceps profundus* was only recorded in *P. hilarii*.

Regarding the muscles for which thin sections include origin and insertion attachment sites (i.e. *m. subscapularis*, *m. deltoideus* and *m. coracobrachialis brevis*), Sharpey's fibers were recorded in all except the insertion of the *m. coracobrachialis brevis*. The *m. subscapularis* presents a different distribution of fibers when comparing its origin and insertion: they are distributed in patches at the origin but are continuously distributed at the area of insertion; this feature was observed in the three species. On the other hand, the *m. deltoideus* presents a different distribution of the fibers at its origin in the three species (the fibers are continuously distributed in *C. chilensis* but in patches in *H. tectifera* and *P. hilarii*); however, Sharpey's fibers are continuously distributed at the insertion of this muscle in the three species. The *m. coracobrachialis brevis* presents Sharpey's fibers at its origin, with a similar distribution in the three species. Finally, in *P. hilarii* and *H. tectifera,* the *m. coracobrachialis magnus* presents fibers continuously distributed at its origin and insertion.

Sharpey's fibers at the insertion of *m. latissimus dorsi*, *m. coracobrachialis*, *m. subscapularis* and *m. pectoralis* have also been observed in other vertebrates, such as *Crocodylus niloticus* (Suzuki et al. 2003). However, we observed fibers at the insertion of the *m. coracobrachialis* only in *C. chilensis*. At the origin of *m. triceps brachii*, *m. deltoideus*, *m. supracoracoideus*, *m. biceps* and *m. flexor carpi radii*, Sharpey's fibers are also observed in *Crocodylus niloticus* (Suzuki et al. 2003).

According to Suzuki et al. (2002), the classification of different muscular insertions could be determined on the basis of the angle at which the Sharpey's fibers penetrate the bone. In this study, it was not possible to adjust this classification to our observations because in many cases the fibers penetrate at different angles along the entire attachment site of one muscle (i.e. attachment of *m. subscapularis* in the acromion of *C. chilensis*, Fig. 9). Also, given that the fibers were distributed in different patterns of densities and orientations, we generated a classification (see Results). The classification includes three types of orientation patterns (I, II and III) and three types of distribution patterns (A, B, C).

Petermann & Sander (2013) stated that the cross-pattern (probably in reference to the Type II pattern here described) is due to the presence of a muscular attachment added to another structure as a tendon or another muscle. We found such a correlation in only a few cases (i.e. the attachment sites of the *m. supracoracoideus anterior* and *m. deltoideus* in the acromion of *H. tectifera*; the attachment sites of *m. triceps brachii* and *m. pectoralis* in the humerus of *P. hilarii*). In specimens examined here, the cross-patterns of Sharpey's fibers are also present in attachment zones where the muscle wraps the bone, offering many points of attachment in one area. In this way, Type II and III patterns were found in attachment sites extended at the most strongly curved area of the bone, as the lateral area of the scapular blade and the ventral area of the acromion.

The turtle bones analyzed here exhibit poorly vascularized or almost avascular cortices (i.e. *C. chilensis* and *H. tectifera*, *P. hilarii*, respectively), so it was not possible to associate the presence or orientation of vascular canals with a muscle attachment. However, in *H. tectifera* we found longitudinal vascular canals together with Sharpey's fibers of the Type II pattern in the attachment site of *m. subscapularis* (Figs 6M and 7A) and *m. supracoracoideus anterior*. Even though a relation between the orientation of vascular canals with a muscular attachment was mentioned for crocodiles and lizards by some authors (Petermann & Sander, 2013), this relation has not yet been clearly observed in turtles (Suzuki et al. 2002, 2003; Petermann & Sander, 2013). However, this lack of relation between Sharpey's fibers and vascular canals could be due to poor vascularization of the cortex in the specimens studied here.

In previous studies, a correlation between the shape and orientation of osteocyte lacunae and the presence of Sharpey's fibers was reported (e.g. in the 'direct unmediated insertion' of crocodilian, Suzuki et al. 2003; and in the in the muscle attachment of the *Eusthenopteron* humerus, Sanchez et al. 2013). In our sample, we only found a similar relation in the tendinous attachment sites of *m. latissimus dorsi* + *m. teres major* (in *C. chilensis*; Fig. 8J) and *m. testocoracoideus* (in *P. hilarii*). In this region, the osteocyte lacunae are flattened and follow the orientation of the Sharpey's fibers. Finally, in particular areas where the Sharpey's fibers were in cross-pattern (Type II and III), abundant, relatively large and osteocyte lacunae without a particular shape were observed.

Sharpey's fibers and muscle attachments

As stated above, the attachment sites of some muscles are more extended in the terrestrial *C. chilensis* than in the freshwater turtles here analyzed. These muscles are principally related to abduction, protraction and rotation of the limb (*m. deltoideus* and *m. subscapularis)* and retraction and adduction of the arm (*m. pectoralis*), which are important in terrestrial locomotion. In contrast, in the freshwater

turtles, the muscles involved in adduction, retraction (*m. supracoracoideus anterior* and *m. coracobrachialis magnus*) and flexion (*m. brachialis inferior*) are larger. Comparing the microstructure of attachment areas of these muscles, we found some specific differences in relation to some muscles.

The major differences between terrestrial and aquatic turtles were observed in the orientation patterns at the attachment site of the *m. deltoideus* and *m. supracoracoideus.* The *m. deltoideus* shows Sharpey's fibers distributed throughout the whole attachment site in *C. chilensis*; however, these are restricted to a patch in *P. hilarii* and *H. tectifera*. In the three species analyzed here, the attachment site of the *m. deltoideus* to the acromion shows the highest concentration of Sharpey's fibers in the dorsal area. However, the orientation patterns of fibers were Type I and Type II in terrestrial and in freshwater species, respectively. Particularly, the Type II fibers in the freshwater turtles might be due to the interaction of two attaching muscles (*m. deltoideus* and *m. supracoracoideus anterior*) in the same area. At the insertion site of this muscle (proximal epiphyses of the humerus), the orientation pattern of Sharpey's fibers was Type II in *C. chilensis* and Type I in the other two species. In relation to the *m. supracoracoideus anterior*, Sharpey's fibers were distributed in patches along the acromial origin of this muscle in the three species. The pattern of orientation was Type I in *C. chilensis* and Type II in *H. tectifera*. As stated above, in terrestrial turtles the *m. deltoideus* serves in the rotation of the pectoral girdle and the humerus, rising and lowering the limb. As a result, the strength of this muscle could be correlated to the presence of Sharpey's fibers in the whole attachment site and with all of the fibers oriented in a Type I pattern. However, in the aquatic turtles in which the *m. supracoracoideus anterior* is implied in pulling the humerus far forward in a propulsive stroke, Sharpey's fibers had a Type II pattern of orientation.

Since the sample number precludes the use of statistical tools, some degree of intraspecific variation cannot be ruled out with regard to the observed variation.

Conclusions

In recent years some studies have focusing on the correlation between myology and osteohistology, analyzing Sharpey's fibers. Since these fibers can be observed both in extant and extinct organisms, the microanatomical information on the muscle attachment is a starting point in morpho-functional and paleobiological studies. Among reptiles, these types of analyses have not been done in turtles. Here we present a comparative study of three species of turtles with different types of locomotion (aquatic vs. terrestrial). Although an increase in sampling is necessary to discern how intraspecific differences can alter the biological interpretations; our results provide novel information that

contributes to the anatomical and histological knowledge about turtles. Our data also allow us to support or review previous observations regarding the relation between bone histology and soft tissues. In this work, we compared our results in turtles with previous work done in other amniotes and we observed some differences (Petermann & Sander, 2013; Sanchez et al. 2013). In this regard, we observed the occurrence of Sharpey's fibers both in tendinous and fleshy attachment sites; the absence of correlation between the vascular canals and the muscular attachment sites; and the apparent absence of correlation between the density of osteocyte lacunae and the muscular attachment sites. On the other hand, we support previous reports that the presence of Sharpey's fibers does not correspond exactly to the total extension of the attachment site of some muscles. We also agree that the different patterns of fibers could correspond to more than one attachment and to different muscle strengths (Hieronymus, 2006; Petermann & Sander, 2013). To organize the information revealed in this work, we classified the density and orientation of Sharpey's fibers. Also, we used the classification to develop an analysis focused on the different locomotor types presented in the species studied here. Muscle reconstruction based on osteological evidence has been considered a useful tool when making muscle inferences. These inferences, which are supported by the study of living organisms, are used to infer paleobiological traits.

Acknowledgements

Author contributions

All the authors participated in the editing of the manuscript. M.E.P. created the figures. M.E.P. and P.B. conducted the myological study and described the results. M.E.P., I.C. and B.D. carried out the osteohistological study and described the results.

References

Aaron JE (2012) Periosteal Sharpey's fibers: a novel bone matrix regulatory system? *Front Endocrinol* **3**, 98.

Abdala V, Manzano AS, Herrel A (2008) The distal forelimb musculature in aquatic and terrestrial turtles: phylogeny or environmental constraints? *J Anat* **213**, 159–172.

Avis V (1959) The relation of the temporal muscle to the form of the coronoid process. *Am J Phys Anthropol* **17**, 99–104.

Benjamin M, Ralphs JR (1997) Tendons and ligaments – an overview. *Histol Histopathol* **12**, 1135–1144.

Benjamin M, Evans EJ, Copp L (1986) The histology of tendon attachments to bone in man. *J Anat* **149**, 89.

Benjamin M, Kumai T, Milz S, et al. (2002) The skeletal attachment of tendons – tendon 'entheses'. *Comp Biochem Physiol A* **133**, 931–945.

Bennett DH, Gibbons JW, Franson JC (1970) Terrestrial activity in aquatic turtles. *Ecology* **51**, 738–740.

Biermann H (1957) Die Knochenbildung im Bereich periostaler-diaphysarer Sehnen- und Bandansätze. Cell Tissue Res **46**, 635–671.

Boyde A (1972) Scanning electron microscope studies of bone. *Biochem Physiol Bone* **1**, 259–310.

Chinsamy A, Raath MA (1992) Preparation of fossil bone for histological examination. *Palaeontol Africana* **29**, 39–44.

Cooper RR, Misol S, Stimmel P (1970) Tendon and ligament insertion: a light and electron microscopic study. *J Bone Joint Surg Am* **52**, 1–170.

Davenport J, Munks SA, Oxford PJ (1984) A comparison of the swimming of marine and freshwater turtles. *Proc R Soc Lond B Biol Sci* **220**, 447–475.

Depecker M, Berge C, Penin X, et al. (2006) Geometric morphometrics of the shoulder girdle in extant turtles (Chelonii). *J Anat* **208**, 35–45.

Felts WJ (1959) Transplantation studies of factors in skeletal organogenesis. I. The subcutaneously implanted immature long-bone of the rat and mouse. *Am J Phys Anthropol* **17**, 201–215.

Francillon-Vieillot H, de Buffrénil V, Castanet J, et al. (1990) Microstructure and mineralization of vertebrate skeletal tissues. In: *Skeletal Biomineralization: Patterns, Processes and Evolutionary Trends*, vol. 1. (ed. Carter JG), pp. 471–530. New York: Van Nostrand Reinhold.

Hems T, Tillmann B (2000) Tendon entheses of the human masticatory muscles. *Anat Embryol* **202**, 201–208.

Hieronymus TL (2002) Microanatomical correlates of muscle attachment and their implications for muscular reconstruction. *Integr Comp Biol* **42**, 1243.

Hieronymus TL (2006) Quantitative microanatomy of jaw muscle attachment in extant diapsids. *J Morphol* **267**, 954–967.

Hoyte DA, Enlow DH (1966) Wolff's law and the problem of muscle attachment on resorptive surfaces of bone. *Am J Phys Anthropol* **24**, 205–213.

Hurov JR (1986) Soft-tissue bone interface: how do attachments of muscles, tendons, and ligaments change during growth? A light microscopic study. *J Morphol* **189**, 313–325.

Jayes AS, Alexander R (1980) The gaits of chelonians: walking techniques for very low speeds. *J Zool* **191**, 353–378.

Jones SJ, Boyde A (1974) The organization and gross mineralization patterns of the collagen fibres in Sharpey's fibre bone. *Cell Tissue Res* **148**, 83–96.

Matyas JR, Bodie D, Andersen M, et al. (1990) The development morphology of a 'periosteal' ligament insertion: Growth and maturation of the tibial insertion of the rabbit medial collateral ligament. *J Orthop Res* **8**, 412–424.

Moss ML (1971) Functional cranial analysis and the functional matrix. *Am Speech Hear Assoc Rep* **6**, 5–18.

Nakajima Y, Hirayama R, Endo H (2014) Turtle humeral microanatomy and its relationship to lifestyle. *Biol J Linn Soc* **112**, 719–734.

Petermann H, Sander M (2013) Histological evidence for muscle insertion in extant amniote femora: implications for muscle reconstruction in fossils. *J Anat* **222**, 419–436.

Rasband W (2003) *Image J*. Bethesda: National Institutes of Health. http://rsb.info.nih.gov/ij/

Rivera AR, Blob RW (2010) Forelimb kinematics and motor patterns of the slider turtle (*Trachemys scripta*) during swimming and walking: shared and novel strategies for meeting locomotor demands of water and land. *J Exp Biol* **213**, 3515–3526.

Rivera AR, Blob RW (2013) Forelimb muscle function in pignosed turtles, *Carettochelys insculpta*: testing neuromotor conservation between rowing and flapping in swimming turtles. *Biol Lett* **9**, 5.

Sanchez S, Dupret V, Tafforeau P, et al. (2013) 3D microstructural architecture of muscle attachments in extant and fossil vertebrates revealed by synchrotron microtomography. *PLoS One* **8**, e56992.

Scott JH (1957) Muscle growth and function in relation to skeletal morphology. *Am J Phys Anthropol* **15**, 197–234.

Staszyk C, Gasse H (2001) The enthesis of the elbow-joint capsule of the dog humerus. *Eur J Morphol* **39**, 319–323.

Suzuki D, Murakami G, Minoura N (2002) Histology of the bone–tendon interfaces of limb muscles in lizards. *Ann Anat* **184**, 363–377.

Suzuki D, Murakami G, Minoura N (2003) Crocodilian bone–tendon and bone-ligament interfaces. *Ann Anat* **185**, 425–433.

Thomopoulos S, Genin GM, Galatz LM (2010) The development and morphogenesis of the tendon-to-bone insertion – What development can teach us about healing. *J Musculoskelet Neuronal Interact* **10**, 35–45.

Trotter JA (2002) Structure function considerations of muscle-tendon junctions. *Comp Biochem Physiol A Mol Integr Physiol* **133**, 1127–1133.

Walker WF Jr (1971) A structural and functional analysis of walking in the turtle, *Chrysemys picta marginata*. *J Morphol* **134**, 195–213.

Walker WF (1973) The locomotor apparatus of Testudines. In: *Biology of the Reptilia vol. 4, Morphology D*. (eds Gans C, Parsons P), pp. 1–99. London: Academic Press.

Washburn SL (1947) The relation of the temporal muscle to the form of the skull. *Anat Rec* **99**, 239–248.

Wyneken J, Witherington D (2001) The anatomy of the sea turtle. In: U.S. Department of Commerce NOAA. Technical Memorandum NMFS-SEFSC-470, pp. 1–172.

Yasukawa Y, Hikida T (1999) Musculus biceps in Testudines, with special reference to its variation in the family Bataguridae. *J Herpetol* **33**, 487–490.

Zug GR (1971) Buoyancy, locomotion, morphology of the pelvic girdle and hindlimb, and systematics of cryptodiran turtles. Museum of Zool., University of Michigan, *Misc Publ* **142**, 1–98.